VOLUME-2
ISSUE-1
2022

e-ISSN: 2791-8335

JOURNAL OF ARTIFICIAL INTELLIGENCE AND DATA SCIENCE

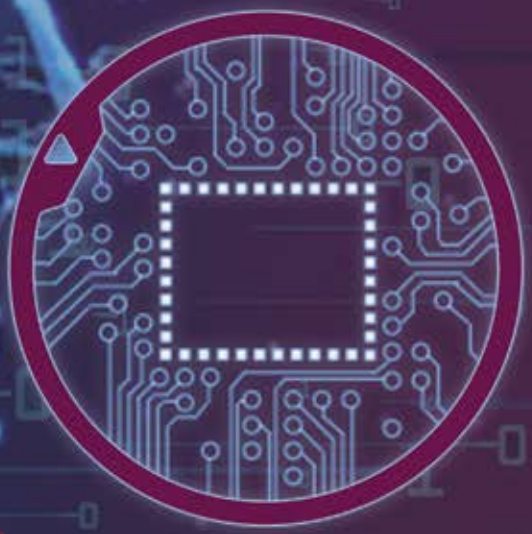

İZMİR KÂTİP ÇELEBİ UNIVERSITY
Artificial Intelligence and Data Science
Research and Application Center

JAIDA

HTTPS://DERGIPARK.ORG.TR/PUB/JAIDA

JOURNAL OF ARTIFICIAL INTELLIGENCE & DATA SCIENCE

Volume 2 – Issue 1 – June 2022 **E-ISSN: 2791-8335**

Aim & Scope

The Journal of Artificial Intelligence and Data Science (JAIDA) is an international, scientific, peer-reviewed, and open-access e-journal. It is published twice a year and accepts only manuscripts written in English. The aim of JAIDA is to bring together interdisciplinary research in the fields of artificial intelligence and data science. Both fundamental and applied research are welcome. Besides regular papers, this journal also accepts research field review articles.

Contact

Web site: https://dergipark.org.tr/pub/jaida
E-mail: ikcujaida@gmail.com
Phone: +90 (232) 329 35 35/3731/ 3808/3819
Fax: +90 (232) 325 33 60
Mailing address: İzmir Katip Çelebi Üniversitesi, Yapay Zeka ve Veri Bilimi Uygulama ve Araştırma Merkezi, Balatçık Kampüsü, Çiğli Ana Yerleşkesi, 35620, İzmir

ÖNSÖZ

Yapay Zeka ve Veri Bilimi alanındaki teknolojik ve bilimsel gelişmeler; Yapay Zekanın endüstri, sağlık, otomotiv, ekonomi, eğitim gibi bir çok farklı alanda uygulanmasına imkan sağlamıştır. Ülkemiz Ulusal Yapay Zeka Stratejisinde; yeni bir çağın eşiğine gelindiği, yapay zekayla üretim süreçleri, meslekler, gündelik yaşam ve kurumsal yapıların yeni bir dönüşüm sürecine girdiği vurgulanarak, Yapay Zekanın öneminden bahsedilmiştir.

Sayın Cumhurbaşkanımızın da belirttiği gibi ülkemiz adına insan odaklı yeni bir atılım yapmanın zamanının geldiğine inanıyoruz. Yapay zeka çağına geçiş noktasında Türkiye'nin lider ülkelerden biri olması motivasyonu ile üniversitemizde yapay zeka teknolojilerinin kullanıldığı projeler gerçekleştirmekte, kongreler ve bilimsel etkinlikler düzenlemekteyiz.

Günümüz dünyasına rengini veren dijital teknolojilerin odağındaki ana unsurun yapay zeka teknolojilerinin olduğu düşüncesi ile yola çıkarak hazırlamış olduğumuz Yapay Zekâ ve Veri Bilimi Dergisinin, Ülkemiz Ulusal Yapay Zeka Stratejisinde belirtilen "Dijital Türkiye" vizyonu ve "Milli Teknoloji Hamlesi" kalkınma hedefleri doğrultusunda katkı sağlayacağı inancındayız.

Dergimizin hazırlanmasında emeği geçen üniversitemiz Yapay Zekâ ve Veri Bilimi Uygulama ve Araştırma Merkez Müdürü, Baş Editör Prof. Dr. Ayşegül ALAYBEYOĞLU'na, Editör ve Danışma kurulu üyelerine, akademik çalışmaları ile sağladıkları destek için tüm yazarlara, hakem olarak görev alan değerli bilim insanlarına teşekkür eder, dergimizin yeni sayısının ülkemize hayırlı olmasını dilerim.

Prof. Dr. Saffet KÖSE, Rektör

Dergi Sahibi

PREFACE

Technological and scientific developments in Artificial Intelligence and Data Science enabled the application of Artificial Intelligence in many different fields such as industry, health, automotive, economy and education. In our country's National Artificial Intelligence Strategy; the importance of Artificial Intelligence was mentioned by emphasizing the transformation process of production processes, occupations, daily life and corporate structures with artificial intelligence.

As stated by our President, we believe that the time has come to make a new human-oriented breakthrough on behalf of our country. With the motivation of Turkey being one of the leading countries at the point of transition to the age of artificial intelligence, we realize projects in which artificial intelligence technologies are used, and organize congresses and scientific events at our university.

We have prepared the Journal of Artificial Intelligence and Data Science with the idea that the main element in the focus of digital technologies that color today's world is artificial intelligence technologies, and we believe that our journal will contribute to the development goals of the "Digital Turkey" vision and "National Technology Move" stated in the National Artificial Intelligence Strategy of our country.

I would like to thank Prof. Dr. Ayşegül ALAYBEYOĞLU, the Director of Artificial Intelligence and Data Science Application and Research Center of our university. I would also like to thank to Editor and Advisory Board members, to all authors for their supports with their academic studies and to reviewers for their contributions to the preparation of our journal. I wish the new issue of our journal to be beneficial for our country.

Prof. Dr. Saffet KÖSE, Rector

Privilege Owner

BAŞ EDİTÖR'DEN

Değerli Araştırmacılar ve Dergi Okuyucuları;

İzmir Kâtip Çelebi Üniversitesi Yapay Zekâ ve Veri Bilimi Uygulama ve Araştırma Merkezi olarak Rektörümüz Prof. Dr. Saffet Köse sahipliğinde Yapay Zekâ ve Veri Bilimi Dergisinin ikinci cilt birinci sayısını sizlerle buluşturmanın gururunu yaşamaktayız.

İzmir Kâtip Çelebi Üniversitesi Yapay Zekâ ve Veri Bilimi Uygulama ve Araştırma Merkezi olarak hedefimiz; Cumhurbaşkanlığı Dijital Dönüşüm Ofisi Başkanlığı ve Sanayi ve Teknoloji Bakanlığı tarafından hazırlanan "Ulusal Yapay Zekâ Stratejisi" hedefleri doğrultusunda dergi, kongre, eğitim, bilimsel etkinlikler ve proje faaliyetleri gerçekleştirerek ülkemizin yapay zekâ alanındaki gelişim sürecine katkı sağlamaktır.

Farklı üniversitelerden, bilimsel disiplinlerden ve alanlardan değerli araştırmacıların İngilizce dilinde hazırlamış oldukları 5 adet araştırma ve 1 adet inceleme makalesi bu sayı kapsamında sunulmaktadır. Siz değerli araştırmacılarımızın destekleri ile kaliteyi daha da arttırarak en kısa sürede ulusal ve uluslararası indekslerde daha çok taranan bir dergi olmayı hedeflemekteyiz.

Dergimizin yayın hayatına başlaması ve tüm merkez faaliyetlerinde büyük desteklerini gördüğümüz başta Rektörümüz Prof. Dr. Saffet KÖSE olmak üzere; dergimize olan destekleri için tüm yazarlara, dergimizin yayına hazırlanmasında heyecanla çalışan ve çok büyük emek harcayan Baş Editör Yardımcılarına, Editör ve Danışma kurulu üyelerimize, hakem olarak görev alan tüm değerli bilim insanlarına en derin şükranlarımı sunarım.

Saygılarımla,

Prof. Dr. Ayşegül ALAYBEYOĞLU

Baş Editör

LETTER FROM THE EDİTOR-IN-CHIEF

Dear Researchers and Readers of the Journal,

As İzmir Katip Çelebi University Artificial Intelligence and Data Science Application and Research Center, we are proud to present you the volume 2 issue 1 of the Journal of Artificial Intelligence and Data Science (JAIDA), hosted by our Rector Prof. Dr. Saffet Köse.

As İzmir Katip Çelebi University Artificial Intelligence and Data Science Application and Research Center, our goal is; to contribute to the development process of our country in the field of artificial intelligence by carrying out journals, congresses, education, scientific events and project activities in line with the objectives of the "National Artificial Intelligence Strategy" prepared by the Digital Transformation Office of the Presidency of Türkiye and the Ministry of Industry and Technology.

5 research and 1 review articles prepared by valuable researchers from different universities, scientific disciplines and fields are presented within the scope of this issue. With the support of esteemed researchers, we aim to increase the quality even more and become a journal that is scanned in national and international indexes more as soon as possible.

I would like to express my deepest gratitude to Our Rector, Prof. Dr. Saffet KÖSE, who supported the publication of our journal and the research center's activities; to all the authors for their support to our journal; to our Associate Editors, who worked enthusiastically and put great efforts into the preparation of our journal; to our Editorial and Advisory Board members, and all esteemed scientists who served as reviewer.

Best Regards,

Prof. Dr. Ayşegül ALAYBEYOĞLU

Editor-in-Chief

CONTENTS

Journal of Artificial Intelligence and Data Science (JAIDA)
e-ISSN: 2791-8335
https://dergipark.org.tr/pub/jaida

Vol. 2, No. 1, pp. 1-7, 2022
Research Article

Depth Perception Assessment of a 3D Video Based on Spatial Resolution

Gokce NUR YILMAZ[1,*], Yucel CIMTAY[1]

[1]TED University, Faculty of Engineering, Department of Computer Engineering, Turkey

Abstract
Burgeoning advances in 3 Dimensional (3D) video technologies can only be emphasized by considering the impact of these technologies on the perception of 3D videos from a user point of view. It is only possible to do this by considering the key factors that characterize the nature of a 3D video. Under the light of this fact, spatial resolution and perceptually significant depth levels, which are two effective factors for the depth perception of a 3D video, are used to develop a Reduced Reference (RR) model for the depth perception prediction of a 3D video. While determining the perceptually significant features, bilateral (abstraction) filter is exploited in this study. Structural SIMilarity metric (SSIM) is used to predict the depth perception enabled considering the degradation in the perceptually important features of depth maps having different spatial resolutions. The performance results of the developed model prove that it is quite effective in the depth perception prediction of a 3D video.
Keywords: 3D video; depth perception prediction; spatial resolution.

1. Introduction

Recent advances in 3 Dimensional (3D) video technologies enable 3D video multimedia services to provide better viewing experience to heterogeneous end-users. 3D video coding, transmission, adaptation are the frequently used names to these 3D video technologies. This viewing experience can be improved by investigating the depth perception assessment results of the end-users as feedback to modify the 3D content and service parameters. In order to make these parameters more reliable, the depth perception should be predicted as the most reliable way as possible [1]-[4].

In the current situation, the depth perception can be reliably assessed using subjective evaluation experiments. These experiments use human observers while assessing the depth perception of a 3D video. Therefore, they are considered quite effective for the depth perception assessment. However, they also cause costs in terms of money and time. There is also another way of assessing the depth perception of a 3D video in the literature namely objective model based assessment. The objective models can enable evaluation results in iterative and robust ways. Full Reference (FR), Reduced Reference (RR) and No Reference (NR) [1]-[3] are three objective model types. In the literature, there are objective model types developed for the depth perception assessment. The objective models developed for the video quality assessment of 2 Dimensional (2D) videos ((i.e., Peak-Signal-to-Noise-Ratio (PSNR) [5], Structural SIMilarity (SSIM) [6] and Video Quality Metric (VQM) [7]) are integrated with the results of the subjective experiments conducted for the depth perception evaluation in [8]. In [9], in order to develop a FR objective model for the depth perception assessment of a 3D video, first of all, subjective experiments are carried out to evaluate the sensitivity of the Human Visual System (HVS) towards binocular disparity, relative size, retinal blur is evaluated using the subjective experiments. Following this, a FR metric is developed for measuring the depth perception of a 3D video. When considering an FR assessment model, both the original and compressed videos are required at the end-user side. This can cause operational difficulties for the depth perception assessment. Therefore, the NR and RR metric types can be used alternatively to the FR metric type for assessing the depth perception of a 3D video. The depth range, vertical misalignment, and temporal consistency parameters are used to propose a NR depth perception model in [10]. In [11], the binocular disparity, region of depth relevance, frame based feature extraction and temporal information are exploited for the depth perception prediction in terms of a NR manner. In [3], a NR depth perception metric integrating binocular parallax, lateral motion, and aerial perspective cues for predicting perceived depth from the view of users is proposed. In [12], a RR model is proposed for the depth perception by extending the SSIM using edge information. It is a fact that a NR model does not need an original video during the assessment process.

Nevertheless, while evaluating the depth perception in the RR metric type, extra information extracted from the original and/or compressed 3D videos are needed. Thus, it can be stated that the RR models can provide more robust 3D video quality assessment than the NR metrics. However, in the literature, there is a lack of a reliable, efficient, and effective RR depth perception prediction model. Considering this, a RR model is developed in this study for predicting the depth perception of users towards a 3D video. Color plus depth map 3D video

*Corresponding author e-mail address: gokce.yilmaz@tedu.edu.tr

Received: 08/02/2022; Accepted: 21/02/2022

representation form enabled by a color video and its depth map counterpart has advantages over the other representation forms (e.g., left and right 3D video representation form) in terms of the network usage [1]-[3]. Therefore, the color plus depth map representation form is used while developing the proposed RR model in this study.

While trying to enhance the quality of the depth perception prediction results, key factors contributing the depth perception prediction should also be considered. In the light of this fact, spatial resolution and significant depth level features, which are key factors characterizing the nature of the depth perception [2], are used in the model development process. The significant depth level is a key factor due to the fact that it emphasizes perceptually important features (e.g., edges, shadows, etc.) for the depth perception. Therefore, in order to predict the depth perception of a 3D video, information degradation in the perceptually important features of the depth maps can be quantified. The reason why the spatial resolution is a key feature for the depth perception is that when the spatial resolution increases, the depth perception also improves. The SSIM is exploited to measure the depth perception considering the abstract (i.e., bilateral filtered) original and compressed depth map sequences at different spatial resolutions in this study.

The rest of the paper is organized as follows. The color plus depth map 3D video representation is introduced in Section 2. In Section 3, the proposed model is discussed. The performance assessment results and discussions are presented in Section 4. Finally, Section 5 concludes this study and points to the future work.

2. Color Plus Depth Map 3D Video Representation

Figure 1 [1]-[3] presents a snapshot captured using a 3D depth-range camera generating color plus depth map representation form for a 3D video. As can be observed from the snapshot, the spatial and temporal resolutions of the depth maps are similar to those of their related color images. All of the depth pixels have a related pixel in the color image. These pixels point to the distances of the related color image pixels to the observers. They take grey values from 0 to 255. 0 represents the furthest away pixel while 255 represents the closest pixel to the observers.

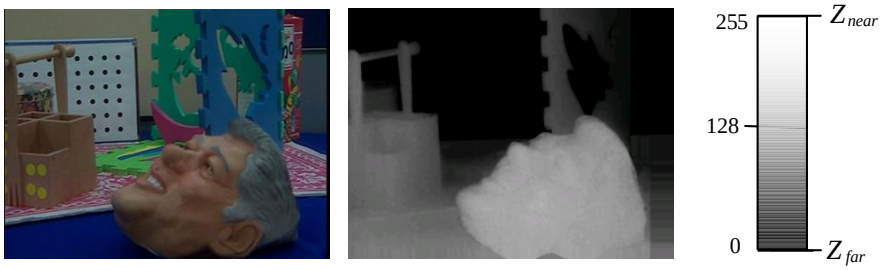

Figure 1. The *Orbi* sequence: (a) Color image (b) Related depth map

In order to render left and right views using the color images and depth maps, Depth-Image-Based Rendering (DIBR) is used. If a color and a depth map exist at the receiver side, a new image can be created by shifting the viewpoint on the screen. Thus, screen parallax is obtained on the screen. As a result of the parallax, different images for the left and right eyes of a viewer are obtained. These images give the depth effect. The basic principle of the DIBR technique relies on calculating screen parallax, which relies on pixel shifting [2]. In order to encode color plus depth stereoscopic video, the conventional 2D encoding techniques can be used [1]-[4].

3. Proposed Model

The proposed metric relies on the framework presented in Figure 2. As can be observed from the figure, the first step of developing the proposed metric is to abstract the original and compressed depth map sequences having different spatial resolutions. Quarter Common Intermediate Format (QCIF: 176×144 pixels), Common Intermediate Format (CIF: 352×288 pixels), and Standard Definition (SD: 704×576 pixels) are exploited as spatial resolutions in this study. In order abstract the depth map sequences at these spatial resolutions, the low contrast regions are simplified whereas the high contrast regions are emphasized using bilateral (abstraction) filter. In this way, the information meaningful for the depth perception assessment of the 3D video (e.g., the edges and shadows) is emphasized [1]-[3]. The bilateral filter utilizes Gaussian filtering method to replace each pixel value of an image with a weighted average of neighborhood pixel values. In this way, the image is smoothened using edge-preserving and noise reduction [12]. The bilateral filter is computed for a pixel using the equation below [1]:

$$F_a = \sum_{b\in\beta} w_{ab}(I_b / \sum_{b\in\beta} w_{ab}) \quad (1)$$

where, a is a pixel, I_b is at the intensity of pixel b in the kernel neighborhood β. The weighting coefficient at pixel b is computed as follows [2]:

$$w_{ab} = c(a,b)s(a,b) \quad (2)$$

where, $c(a,b)$ and $s(a,b)$ are clossiness and similarity kernel filters, respectively. These kernel filters are calculated as follows [3-4]:

$$c(a,b) = e^{(\frac{-1}{2}(a-b)^2/\sigma_c{}^2)} \quad (3)$$

$$c(a,b) = e^{(\frac{-1}{2}(a-b)^2/\sigma_c{}^2)} \quad (4)$$

Figure 3 presents the snapshots of the abstracted Breakdance and Chess depth map sequences. As seen from the figure, the perceptually important features in the abstracted depth map sequences are perceived better.

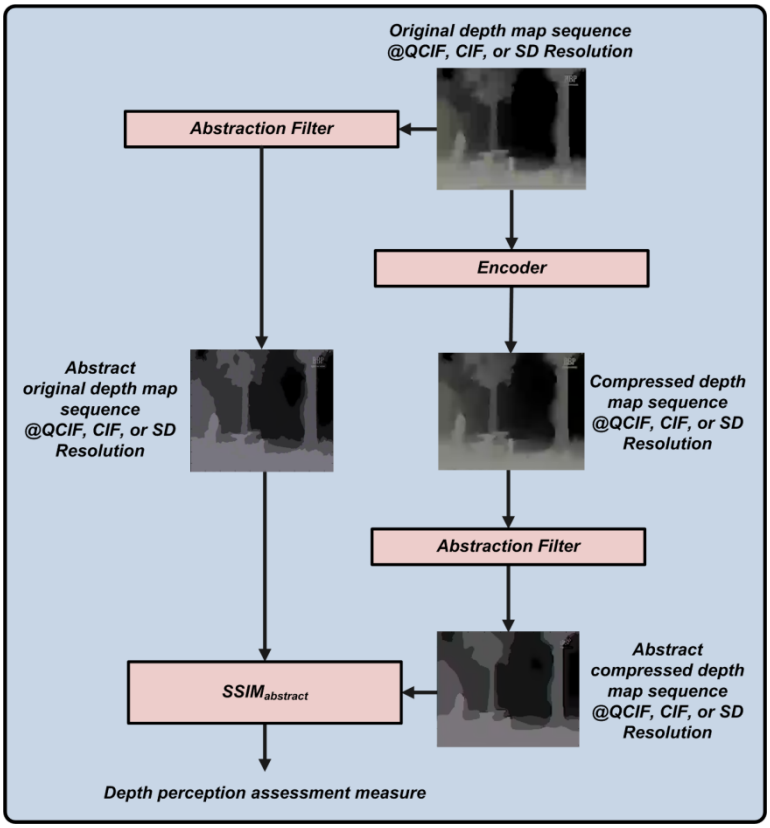

Figure 2. The framework of the proposed model

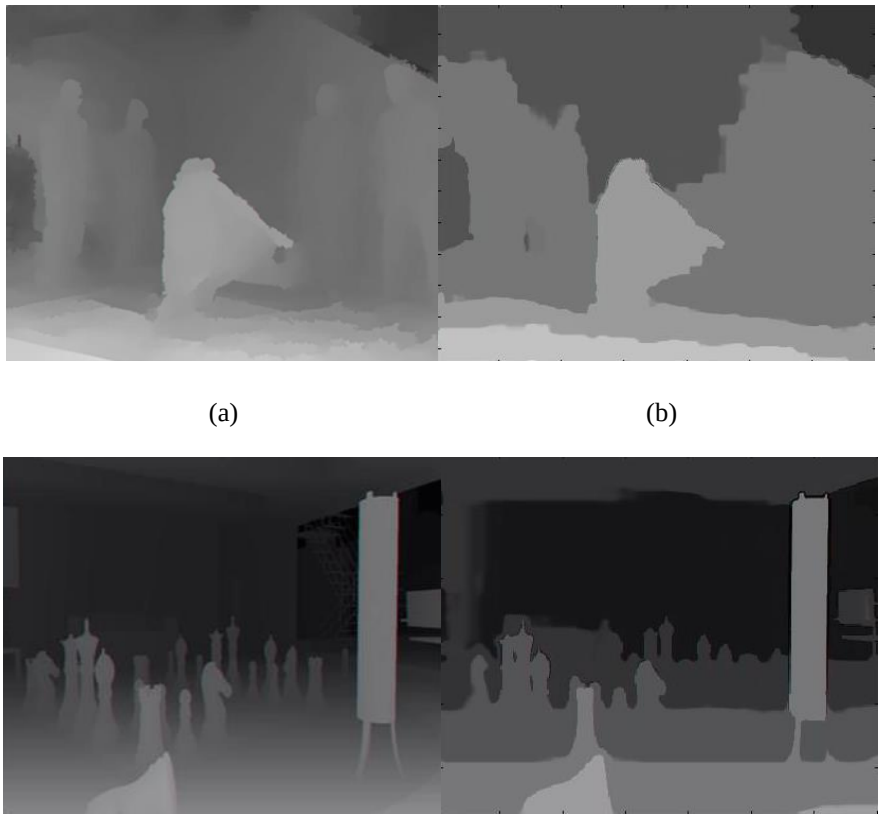

(a) (b)

(b) (d)

Figure 3. Abstracted Breakdance and Chess depth map sequences

As can also be seen from Figure 2, the last step of the proposed metric development is to utilize the SSIM to predict the performance of the proposed RR metric by comparing the abstracted information between the original and compressed depth map sequences at different spatial resolutions. $SSIM_{abstract}$ in Figure 2 refers to the SSIM measurement for the side information (i.e., the abstract original depth map sequence at QCIF, CIF, or SD spatial resolution) in the RR metric. The SSIM exploits the structural distortion of a distorted video compared to the original one. Thus, it is efficient to measure the degradation in the perceptually important features.

4. Results and Discussions

Three original 3D videos namely: Ice, Eagle, and Chess are used to derive the performance evaluation results. The snapshots of these 3D video sequences are illustrated in Figure 4. The original 3D video sequences are scaled down from their original resolutions (i.e., 1024×768 pixels) to QCIF, CIF, and SD resolutions using the Advanced Video Coding (AVC) 4-tap half-sample interpolation filter [13]. Four different bit rates (i.e., 512, 768, 1024, and 1536 kbps) are used to encode these down-scaled sequences with the Joint Scalable Video Model (JSVM) reference software version 9.13.1 at 25 fps [14]. 20% of the target bit rate is used to encode the depth map sequences whereas the 80% of the total bit rate is allocated for the color sequences of the 3D videos.

Then, subjective experiments are conducted using these encoded 3D video sequences. Double Stimulus Impairment Scale (DSIS) method is exploited during the experiments as suggested in International Telecommunication Union-Recommendation (ITU-R) BT-500.13 standard [15]. The 3D video sequences are presented in pairs: the first video is the original and the second video is the compressed one in this method. The participants are asked to evaluate the depth perception by comparing the impaired 3D videos with the original ones. During the experiments, an evaluation scale ranging from 1 to 5, which represents the lowest and highest depth perception respectively, is exploited for rating the 3D video sequences.

A 42” Philips multi-view auto-stereoscopic display, which has a resolution of 1920 × 1080 pixels, is utilized while displaying the 3D video sequences. 18 viewers (7 females and 11 males) volunteered in the experiments. Their ages range from 19 to 37 and they are all non-expert viewers. The outliers are omitted after obtaining the experiment results. Then, the Mean Opinion Scores (MOSs) and confidence intervals are computed exploiting 16 volunteers.

The VQM and $SSIM_{abstract}$ results of each 3D video sequence are computed for each bit rate (i.e., 512, 768, 1024, and 1536 kbps) at each spatial resolution (i.e., QCIF, CIF, and SD) considered in this study. The relationship between the MOS, VQM, and $SSIM_{abstract}$ results are approximated considering the symmetrical logistic function as suggested in ITU-R BT.500-13 [15]. The formulation of the symmetrical logistic function is shown in equation 5. [1][2]:

$$s = \frac{1}{1 + e^{(D-D_M)G}} \tag{5}$$

where, s is the normalized opinion score, D is the distortion parameter, and DM and G are constants.

(a)

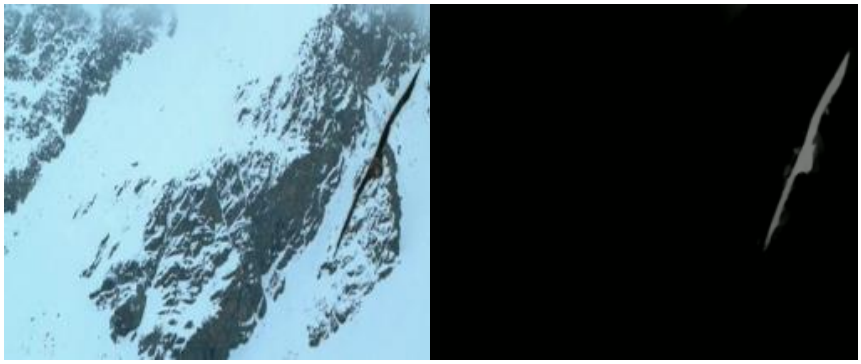

(b)

(c)

Figure 4. Color texture and associated depth map of the (a) Ice (b) Eagle (c) Chess 3D videos

Considering the results of the symmetrical logistic function, Correlation Coefficient (CC), Route Mean Squared Error (RMSE), and Sum of Squares due to Error (SSE) metrics are computed to compare the performances of the MOSs, VQM, and $SSIM_{abstract}$. The CC, RMSE, and SS present the strength of the correlation

between two variables, differences between the predicted values, and how well the correlation is calculated, respectively. The CC, RMSE, and SSE take values between 0 and 1. CC=1, RMSE=0, and SSE=0 present perfect results. The CC, RMSE, and SSE results of each 3D video sequence at each encoded bit rate (i.e., 512, 768, 1024, and 1536 kbps) are averaged for each spatial resolution (i.e., QCIF, CIF, and SD) as illustrated in Table 1.

As can be observed from the CC, RMSE, and SSE results in Table 1, the proposed metric perform better than those of the VQM for each of the spatial resolution. For instance, for the Ice video, VQM for the QCIF take 0.851, 0.07, and 0.175 CC, RMSE, and SSE values, respectively. However, the proposed metric enable a CC result of 0.903, a RMSE result of 0.041, and a SSE result of 0.147 for the QCIF spatial resolution of the Ice video. These outperforming results can also be observed for the rest of the spatial resolutions and videos.

Moreover, as can also be observed from Table 1, the proposed metric's performance gets better when the spatial resolution increases. In other words, the higher the spatial resolution of the depth map is, the better the abstraction result is. The reason behind this is that as discussed in Section 2 related to Figure 3, when the spatial resolution of the depth map sequences enhances, the visualization of the perceptually significant features also increases. Thus, it can be envisaged that the high spatial resolution abstracted depth maps particularly enhance the feeling of immersion into the scenes, which in turn affect the depth perception. These observations present the effectiveness of the proposed RR metric for assessing the depth perception of the 3D video.

Table 1. The performance evaluation results of the proposed model

3D Video	Depth Perception Metric At Different Spatial Resolutions	Depth Perception Results at Different Spatial Resolutions		
		CC	RMSE	SSE
Ice	VQM for QCIF	0.851	0.071	0.175
	VQM for CIF	0.869	0.063	0.169
	VQM for SD	0.883	0.056	0.162
	Proposed Metric for QCIF	0.903	0.041	0.147
	Proposed Metric for CIF	0.912	0.035	0.139
	Proposed Metric for SD	0.934	0.028	0.131
Eagle	VQM for QCIF	0.849	0.083	0.186
	VQM for CIF	0.864	0.074	0.177
	VQM for SD	0.871	0.067	0.171
	Proposed Metric for QCIF	0.908	0.049	0.153
	Proposed Metric for CIF	0.919	0.042	0.144
	Proposed Metric for SD	0.926	0.037	0.138
Chess	VQM for QCIF	0.843	0.088	0.193
	VQM for CIF	0.859	0.085	0.189
	VQM for SD	0.866	0.073	0.182
	Proposed Metric for QCIF	0.901	0.057	0.157
	Proposed Metric for CIF	0.909	0.051	0.149
	Proposed Metric for SD	0.917	0.044	0.143

5. Conclusions

In this paper, an RR metric has been proposed to predict the depth perception of the 3D video sequences. The color plus depth-map representation of the 3D video has been exploited in the proposed RR metric. The proposed RR metric considers the perceptually important depth levels and spatial resolution, which are key factors contributing to the nature of the 3D video, to measure the depth perception in a reliable, efficient, and effective way. The performance evaluation results of the proposed metric prove this fact. It has been envisaged that the development of the 3D video technologies in the consumer electronics market can be accelerated by exploiting the proposed metric. In our future study, the proposed metric will be integrated with a color video perception metric. In this way, both the video quality and depth perception parts of a 3D video perception will be considered.

Declaration of Interest

The authors declare that there is no conflict of interest.

Acknowledgements

This work has been supported by the Scientific and Technological Research Council of Turkey, Project Number: 114E551.

References

[1] G. Nur Yilmaz and F. Battisti, "Depth Perception Prediction of 3D Video for Ensuring Advanced Multimedia Services," IEEE 3DTV Conference: The True Vision - Capture, Transmission and Display of 3D Video, Stockholm-Helsinki, Sweden-Finland, 3-5 June 2018.

[2] G. Nur and G. Bozdagi Akar, "An Abstraction Based Reduced Reference Depth Perception Metric for 3D Video," International Conference on Image Processing (ICIP), Orlando, Florida, USA, 30 September-3 October 2012.

[3] G. Nur Yilmaz, "A Novel Depth Perception Prediction Metric for Advanced Multimedia Applications," Springer Multimedia Systems, 2019.

[4] Perkis et.al., "QUALINET White Paper on Definitions of Immersive Media Experience (IMEx)," arXiv:2007.07032, 2020.

[5] Huynh-Thu and Ghanbari, "Scope of validity of PSNR in image/video quality M. assessment," IET Electronics Letters, vol. 44, no. 13, pp. 800–801, Jun. 2008.

[6] Z. Wang, L. Lu, and A. C. Bovik, "Video Quality Assessment Based on Structural Distortion Measurement," Proc. of Signal Processing: Image Com., vol. 19, no. 2, pp. 121-132, Feb. 2004.

[7] M.H. Pinson and S. Wolf, "A New Standardized Method for Objectively Measuring Video Quality," IEEE Trans. Broadcasting, vol. 50, no. 3, pp. 312-322, Sep. 2004.

[8] D. Kim, D.Min, J. Oh, S. Jeon, and K. Sohn, "Depth Map Quality Metric for Three-Dimensional Video," SPIE Stereoscopic Displays and Applications, San Jose, CA, USA, 18 Jan. 2009.

[9] D.V.S.X De Silva., G. Nur, E. Ekmekcioglu, and A. Kondoz, "QoE of 3D Media Delivery Systems," Media Networks: Architectures, Applications, and Standards, CRC Press Taylor and Francis Group, May 2012.

[10] P. Lebreton, A. Raake, M. Barkowsky, P. Le Callet, "Evaluating Depth Perception of 3D Stereoscopic Videos," IEEE Journal of Selected Topics in Signal Processing, vol.6, pp. 710-720, October 2012.

[11] T.E.R. Chaminda and M. G. Martini, "Quality Evaluation for Real-Time Video Services," IEEE international Conference on Multimedia and Expo, 11-15 July 2011.

[12] G. Nur, S. Dogan, H. Kodikara Arachchi, and A.M. Kondoz, "Impact of Depth Map Spatial Resolution on 3D Video Quality and Depth Perception," IEEE 3DTV Conference: The True Vision - Capture, Transmission and Display of 3D Video, Tampere, Finland, 7-9 June 2010.

[13] Advanced Video Coding for Generic Audiovisual Services, ITU-T Rec. H.264 (03/2005) Std., MPEG-4 AVC/H.264 Video Group.

[14] JSVM 9.13.1. CVS Server [Online]. Available Telnet: garcon.ient.rwth aachen.de:/cvs/jvt

[15] ITU-R BT.500–11, Methodology for the subjective assessment of the quality of television pictures.

Journal of Artificial Intelligence and Data Science (JAIDA)
e-ISSN: 2791-8335
https://dergipark.org.tr/pub/jaida

Vol. 2, No. 1, pp. 8-15, 2022
Research Article

Prediction of Remaining Useful Life for Plastic Injection Molding Machines Using Artificial Intelligence Methods

Gözde ASLANTAS [1,*], Mustafa OZSARAC [1], Merve RUMELLI [1], Tuna ALAYGUT [1], Gözde BAKIRLI [1], Derya BIRANT [2]

[1] VESTEL Electronics, Turkey
[2] Dokuz Eylul University, Engineering Faculty, Department of Computer Engineering, Turkey

Abstract
Sustaining productivity with guaranteed machine availability is of the utmost significance while reducing costs. With the rising technology and the collected data in the industry, accomplishing such a goal is not fictional anymore. This paper proposes an artificial intelligence-based model that predicts the remaining useful life (RUL) of the plastic injection molding machines before requiring maintenance. Data collected from machines in production via sensors is preprocessed by performing various techniques, and anomalies in the data are detected and cleaned. Based on the historical data, the RUL of the machine, which is the duration until maintenance is required, is calculated, and the data is labeled with the RULs accordingly. In the proposed method, the labeling step is followed by feature engineering where the useful features are extracted from the raw data, such as entropy, peak to peak, and crest factor. A feature selection method is also applied to determine their contribution to the estimation accuracy of the RULs. As a comparison, we experimented with various regression models along with various evaluation metrics. The experimental results showed that our proposed approach achieved around 98% in the R^2 performance metric.
Keywords: Artificial intelligence; manufacturing; plastic injection molding machines; predictive maintenance; regression; remaining useful life.

1. Introduction

Any failures and outages of machines in industrial areas will result in a degradation in production, and hence significant costs and penalties in procurement. Maintenance is the key activity in manufacturing, in terms of its impact on cost reduction, and prolonging the life of equipment parts in a reliable way. The main goal of the maintenance activities is to maximize the durability of the machines while minimizing the cost of downtime in production, thus ensuring reliability and continuity in procurement.

Maintenance strategies can be divided into three categories [1] by common usage:

1. *Run-to-failure maintenance* (R2F): Run-to-failure maintenance, which is also called reactive or corrective maintenance, is the simplest approach as it aims to repair the machine or the system after the failure occurred.
2. *Preventive maintenance* (PvM): Preventive maintenance is employed on a scheduled basis in order to prevent any failures without taking into account the health statuses of the machines. This regular maintenance usually prevents failures before it occurs as it aims to but causes additional cost when it is performed unnecessarily.
3. *Predictive maintenance* (PdM): Predictive maintenance is performed as a result of a prediction mechanism based on the historical maintenance data or health states in order to act prior to any failures in the system.

Based on the requirements, each of these maintenance types have different benefits and disadvantages. Negligence of any type of maintenance may result in costly failures, performance issues, and thus production impediments. The frequency and timing of the maintenance are substantial though. Regardless of the health status of the machines, repetitive and non-optimized maintenance can increase the cost as the remaining useful life (RUL) of the machine is not being used effectively. Postponing the maintenance till the time for a machine approaches to zero may also lead to unexpected consequences which will be more costly. Based on the foreseen impacts, utilization of RUL is the most highlighted objective in order to perform sustainable maintenance with long-running equipment.

With the recent advancements in artificial intelligence, big data techniques, and the internet of things (IoT), predictive maintenance (PdM) has become an indispensable part of the new industrial era. PdM involves sensor data monitoring, data-driven condition review, fault diagnosis, fault alerts, and so on. As a benefit of PdM, in comparison with other strategies, the state of the system is observed and evaluated in real-time based on certain parameters of the system. Hence, a system-specific determination is done.

*Corresponding author e-mail address: gozde.aslantas@vestel.com.tr

Received: 14/04/2022; Accepted: 24/05/2022

In this study, predictive maintenance is exploited to determine the RULs of the plastic injection molding machines. Plastic injection molding is a sequential process where plastic is melted, pressed into the mold, cooled to solidify, and removed from the mold as a three-dimensional shape. This process is applied in industrial areas using plastic injection molding machines in two stages: Injection, and Clamping. As a final product, the plastic injection molding machines produce various components such as TV components (i.e., TV cabinets, and stand bases), and plastic components of mobile phones.

In this study, an artificial intelligence-based model is designed and developed by applying machine learning methods to provide the following important benefits:

- To decrease plastic injection molding machine downtime
- To reduce the number of major repairs
- To better management of plastic injection molding machines
- To reduce maintenance costs and operational risk, and so, save money
- To improve safety
- To increase efficiency
- To discover knowledge related to various plastic injection molding machine downtime problems

The main contributions of this paper can be summarized as follows. (i) It proposes an artificial intelligence-based model that accurately predicts the remaining useful life for plastic injection molding machines in the manufacturing industry. (ii) It compares different regression algorithms to determine the best one for predictive maintenance: random forest regression, decision tree regression, and extreme grading boosting regression. (iii) Our study is original in that it extracts useful features (i.e., entropy, peak to peak, and crest factor) from raw data by aggregating samples within a certain time period.

The paper is organized as follows. Section 2 gives a review of related work in the literature. Section 3 explains the proposed approach and the materials used in the study. Section 4 covers the description of the dataset and the experimental details along with the results. Section 5 presents the conclusion and our final thoughts about future work.

2. Literature Review

Remaining useful life (RUL) is the time between a machine's current working state and its failure. RUL prediction is the attempt to estimate the remaining period of normal operation at a particular level of performance for an electronic machine or motor. RUL prediction helps managers to assess the health of machines and to make a maintenance schedule. RUL prediction has been studied in many different areas such as manufacturing [2], energy [3], automotive [4], industry [5], aviation [6], and marine [7].

Selecting the most appropriate machine learning (ML) algorithm is a big challenge for the RUL prediction. Table 1 presents the previous work related to the RUL prediction. In the literature, various ML methods have been explored in the field of predictive maintenance such as Extreme Learning Machine (ELM) [3], Relevance Vector Machine (RVM) [3], Linear Regression (LR) [8], Support Vector Machine (SVM) [9], Multi-Layer Perceptron (MLP) [10, 11], Particle Swarm Optimization (PSO) [12], Decision Tree (DT) [13], and K-Nearest Neighbors (KNN) [14]. Furthermore, ensemble learning methods have been used for RUL prediction such as Random Forest (RF) [8], Gradient Boosting (GBoost), and Extreme Gradient Boosting (XGBoost) [5, 15]. Hence, both bagging and boosting approaches have been tested for predictive maintenance. Moreover, deep learning methods have been applied successfully for the prediction of RUL such as Convolutional Neural Network (CNN), Long Short-Term Memory (LSTM), Recurrent Neural Network (RNN) [16], and Deep Neural Network (DNN) [13].

Some previous studies [11, 15] focused on classification tasks to estimate whether a machine will fail within a certain period of time. On the other hand, most previous works [2-4, 6, 7, 9, 10, 12, 16] performed a regression task to predict the RUL of equipment as a numerical value. Besides, several studies [8, 13, 14] have addressed both classification and regression tasks to solve the RUL prediction problem.

To evaluate the performance of the classification models, they used Accuracy (ACC), Precision (P), Recall (R), F1-Score (F), and Area Under Curve (AUC) metrics. On the other hand, the error evaluation of regression models was analyzed based on the Root Mean Squared Error (RMSE), Mean Squared Error (MSE), Mean Absolute Percentage Error (MAPE), and Coefficient of Determination (R^2).

Our work differs from the aforementioned studies in several aspects. First, we investigated the use of different regression algorithms to predict the RUL of plastic injection molding machines. Second, in the data preprocessing step, we extracted useful features (i.e., entropy, peak to peak, and crest factor) from raw data by aggregating samples within a certain time period.

Table 1. *Related studies (C: Classification R: Regression)*

Reference	Year	ML Algorithms	Task		Application	Evaluation	Sector
			C	R			
Zhao and Liu [2]	2022	CNN		√	Estimating RUL for bearings under different conditions and platforms	RMSE	Manufacturing
Yao et al. [3]	2022	PSO-ELM-RVM		√	Predicting RUL for lithium-ion batteries	RMSE, MAPE	Energy
Chen et al. [4]	2022	SVM		√	Prediction of RUL for fuel cell electric vehicle	MSE, MAPE	Automotive
Böttjer et al. [5]	2022	XGBoost	√		Predicting of RUL for moulds	ACC	Industry
Peng et al. [6]	2021	LSTM, CNN, RF, SVM		√	Predicting RUL for turbofan engine	RMSE	Aviation
Folcaner et al. [7]	2021	SVM, MLP, RF		√	Predicting RUL for fibre ropes	RMSE, R^2	Marine
Wu et al. [8]	2021	CNN, LSTM, LR, SVM	√	√	Prediction for tool wear in shaft production line	ACC, RMSE	Manufacturing
Ragap et al. [9]	2021	SVM, RF, GBoost, CNN, LSTM		√	Prediction of RUL of industrial equipment	RMSE	Industry
Kang et al. [10]	2021	MLP		√	Prediction of the failure of equipment in production lines	MSE	Manufacturing
Orru et al. [11]	2020	MLP, SVM	√		Fault prediction of a centrifugal pump (1: RUL<168, 0: otherwise)	ACC, P, R, F, AUC	Oil and Gas Industry
Bala et al. [12]	2020	RNN, LSTM, PSO		√	Predicting faults in airplane engines	MSE	Aviation
Utah and Jung [13]	2020	SVM, KNN, DT, RF, DNN	√	√	Fault state detection and RUL prediction in alternating solenoid-operated valves	ACC, P, R, F, MAE, MSE, RMSE	Nuclear Eng.
Trinh and Kwon [14]	2020	MLP, KNN, SVM, RF	√	√	Fault-type classification and RUL prediction	MSE, F	Manufacturing
Calabrese et al. [15]	2020	GBoost, RF, XGBoost	√		Prediction of RUL of woodworking machines (30, 20, 10-day RUL)	ACC, P, R, AUC	Industry
Zhang et al. [16]	2020	CNN, SVM, MLP, RNN, LSTM		√	Prediction of RUL of rotatory machine	MAE, RMSE	Manufacturing

3. Material and Methods

The remaining useful life is the time interval in which a machine, component, or motor can be used before it should be repaired or replaced. RUL prediction is useful to determine the machine or component maintenance time reasonably, reduce the accident probability, and improve manufacturing efficiency. RUL prediction is a challenging task due to the lack of an accurate predictive maintenance model.

In this study, we approached the RUL prediction of plastic injection molding machines as a regression problem. Figure 1 shows the general structure of the proposed approach. In the first step, sensor values and the maintenance date of the machines are collected, transferred, and stored in a cloud platform. In the data preparation step, raw data is transformed into a format where the sensor names and the timestamp that indicates the maintenance time are columns and renamed to parameters for machines. RUL for each timestamp when a collection of sensor values is calculated based on the maintenance/failure date. Missing values are eliminated and outliers are detected. Feature selection is performed based on the contribution of the features to the regression problem using several techniques, including random forest regression, permutation, and SHapley Additive exPlanations (SHAP). In addition, data is hourly aggregated using statistical methods such as min, max, mean, standard deviance, skewness, kurtosis, peak to peak, velocity, and entropy. In the training step, the most commonly-used regression methods are applied for benchmarking. As the main performance metric, the coefficient of determination (R^2) metric is used to measure how well the applied method fits the data. RUL prediction is performed by using the model for a new observation. In the next stage, the prediction results are presented to the user via an application for giving feedback about the RUL of the machine. Finally, the output of the model is taken into consideration by a manager for decision-making. Hence, an artificial intelligence-based model is designed and developed by applying machine learning methods to provide significant benefits such as reducing machine downtime, decreasing repair costs, improving efficiency, and increasing safety.

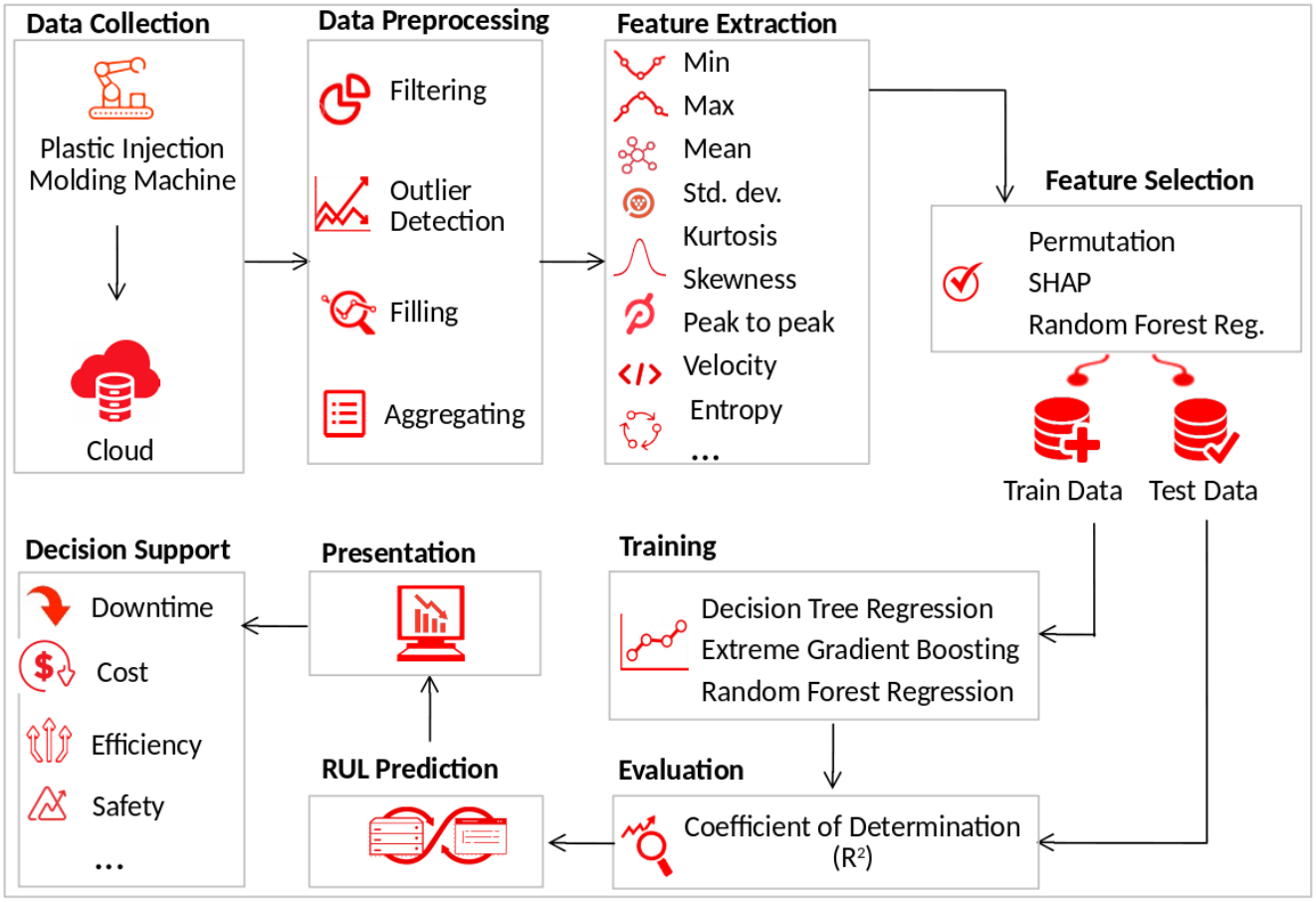

Figure 1. *The general structure of the proposed approach.*

In this study, the most common regression algorithms were used to construct a machine learning model for predictive maintenance: decision tree regression, extreme gradient boosting, and random forest regression. The description of these algorithms is given in Sections 3.1, 3.2, and 3.3, respectively.

3.1. Decision tree regression

The decision tree is one of the most commonly-used supervised learning algorithms utilized in both classification and regression problems. In this method, the inputs are split into nodes, and each node is branched into internal nodes until the leaf nodes. Thus, the input space is divided into non-overlapping nodes where each leaf node maps the input space to the corresponding target. In classification problems, the target variables belong to a discrete set of values while, in regression, they can take real numbers. In this study, a decision tree is applied to build a regression tree.

3.2. Extreme gradient boosting

Extreme gradient boosting (XGBoost) is an ensemble learning algorithm that is based on boosting the various number of decision trees by using gradient descent to optimize them when new decision trees are added to train and combining the estimates with the majority voting for classification or weighted sum for regression problems. It is a popular algorithm since it can handle different machine learning challenges. Its high performance in predictive maintenance has been reported in the literature [15].

3.3. Random forest regression

Random forest is an ensemble learning algorithm that constructs various numbers of decision trees, and the final estimator is chosen based on majority voting or averaging for classification and regression problems. The splits in the decision trees are performed based on the selected hyperparameters. Actually, random forest is typical bagging (bootstrap aggregating) method that utilizes a decision tree as the base learner. It is forced to consider only a subset m of samples and n of features randomly chosen. In this study, a random forest regressor was used for RUL prediction.

4. Experimental Studies

In this study, experimental evaluations of the machine learning methods were performed using real data obtained from plastic injection molding machines. In experimental settings, the grid search method was used for hyperparameter optimization. To validate models, 5-fold cross validation was used. As evaluation criteria, coefficient of determination (R^2) and mean absolute error (MAE) were used. The coefficient of determination or R^2 is the proportion of the total sum of squares between actual values and predicted values, as given in Eq. (1). Based on this evaluation metric, the best model was selected and used for the prediction. MAE depends on the mean of difference among predictions and real values, as given in Eq. (2). A larger R^2 indicates a better model, while a smaller MAE indicates a better prediction performance.

$$R^2 = 1 - \frac{\sum_{i=1}^{n}(O_i - P_i)^2}{\sum_{i=1}^{n}(O_i - P_i)^2} \tag{1}$$

$$MAE = \frac{1}{n}\sum_{i=1}^{n} P_i - O_i \tag{2}$$

where n is the number of samples, P_i is the predicted value, and O_i is the observed value.

4.1. Dataset description and data preparation

Data was collected from a Turkish home and professional appliances manufacturing factory specialized in electronics. The dataset consists of machine name, sensor values, date of collection of sensor data, and maintenance date of three pilot plastic injection molding machines, namely HEP3204, HEP3207, and HEP3213. The size and general information of the raw data with the description of the sensors are presented in Table 2 and Table 3, respectively.

Table 2. *Size and time interval of the raw data.*

Machine Name	Time Interval	Data Size
HEP3204	September 2019 – September 2021	251K
HEP3207	June 2019 – September 2021	205K
HEP3213	May 2018 – September 2021	913K

Table 3. *Description of the sensor data.*

Sensor Name	Description
CLAMPING_FORCE_ACT	Clamping force peak value
CLAMPING_FORCE_SET	Clamping force set value
Closing force-Skx-actual value	Closing force-Skx-actual value
Cycle time-ZUx-actual value	Cycle time-ZU-sets value
HOLD_PRESS_STEP_1-10	Hold pressures between 1st and 10th steps
HYDR_HOLD_PRESS	Hydr. holding pressure peak value
Injection time-ZSx-actual value	Injection time
Material cushion smallest value-CPx-actual value	Material cushion smallest value
OIL_TEMPERATURE	Oil temperature

A pipeline of data preprocessing steps was applied to the raw data. First, the raw data was transformed into a flat table with sensor values, collection date, and maintenance date in columns. The presence of missing values could lead to erroneous results in data analysis and therefore possible errors in solving the regression problem. In order to handle missing or null values in the sensor data, each data attribute that has null values for less than 40% was filled with the result of linear interpolation of the not-missing values at start and end. Data attributes with high missing rates (>40%) and data rows with missing collection date as well were eliminated. After that, RUL was calculated by subtracting the collection date from the maintenance date. Thus, for a set of sensor values collected at a given time period, we added a new numeric column, the RUL value indicating the remaining maintenance time in days. We then removed the sensor collection date and maintenance date from the data as they are used for specifying the RUL value for training data.

Anomalies in data are one of the most significant factors which affect the estimations by causing overfitting or underfitting. Thus, detection of anomalies and dealing with them are essential steps in data preparation. In our study, we detected anomalies based on the z-score limit which was chosen empirically. Z score gives the standard deviations of the data points that are away from the mean which indicates that these data points are outliers. Thus, data with a standard deviation smaller than the specified z-score limit are detected as outliers. We investigated the impact of anomaly detection by performing an ablation study comparing the performance of the proposed approach with two settings: dropping anomalies or keeping them. As seen in Table 4, dropping anomalies from data increases the model performance. While the mean squared error was 10.92 without anomaly detection, it became 2.683 with anomaly detection using z-score. Similarly, the mean absolute error decreased from 1.015 to 0.288 for a plastic injection molding machine when anomaly detection was performed.

Table 4. *Comparative study for anomaly detection*

Score Metric	Without Anomaly Detection	With Anomaly Detection using z-score (z-score limit =4)
Mean Squared Error	10.92	2.683
Mean Absolute Error	1.015	0.288
R^2	0.994	0.998

Data aggregation is an essential part of data analysis that is performed to extract useful features from data and hence, provides a different perspective by enhancing the value of the information. Data rows were aggregated as 1-hour intervals and useful features were extracted for each interval by using statistical techniques, including min, max, standard deviance, mean, absolute mean, median, skewness, kurtosis, entropy, root mean square, peak to peak, crest factor, clearance factor, shape factor, and impulse.

We performed feature selection to emphasize the features that contribute to the regression problem the most, and thus determine the features that will be used in model construction. Feature Importance analysis was performed with the following feature importance techniques:

- *Permutation*: Evaluate the importance of the features when the randomly selected feature is shuffled while others are kept constant by measuring the decrease in the performance of the estimator. The higher value indicates the higher feature importance.
- *SHapley Additive exPlanations (SHAP)*: Evaluate the importance of the features when the randomly selected feature is shuffled while others are kept constant by measuring the contribution magnitude of the features.
- *Random forest feature importance*: Features are evaluated based on the decrease in node impurity where each feature is represented as a node, and the impurity is calculated by taking the probability of the samples that reach the node.

Features in the intersection set of the resulting applications were selected while other features were dropped.

4.2. Experimental results

In this study, various machine learning methods were applied to preprocessed data, and the results were evaluated in terms of R^2 and MAE for comparison. In Table 5, the performance results for each plastic injection molding machine are presented separately. According to the results, it is possible to say that the algorithms had no difficulty in predicting RUL values successfully. Hence, models constructed by tree-based algorithms are prominent models, especially for such regression problems. For example, the random forest algorithm achieved around 99% in the R^2 performance metric for the HEP3204 machine. The comparison in this table depicts that the random forest algorithm outperformed other methods for the HEP3207 machine, achieving the smallest MAE value (0.4615). The MAE results indicate that the proposed models can be successfully used to estimate the remaining useful life of the plastic injection molding machines with low error values.

Table 5. *Performance comparison.*

Algorithms	Coefficient of Determination (R^2)			Mean Absolute Error (MAE)		
	HEP3204	HEP3207	HEP3213	HEP3204	HEP3207	HEP3213
Decision Tree Regression	0.9979	0.9115	0.9860	0.6215	0.6659	1.7586
Extreme Gradient Boosting	0.9978	0.9189	0.9850	0.7033	1.0495	2.5900
Random Forest Regression	0.9948	0.9966	0.9745	1.0157	0.4615	3.4281

Figure 2 shows the average performance comparison of algorithms in terms of R^2. According to the results, the random forest regression algorithm is seen to have better performance than others on average. While RF regressor achieved 0.989 according to the performance metric, XGBoost and DT obtained the values of 0.967 and 0.965, respectively.

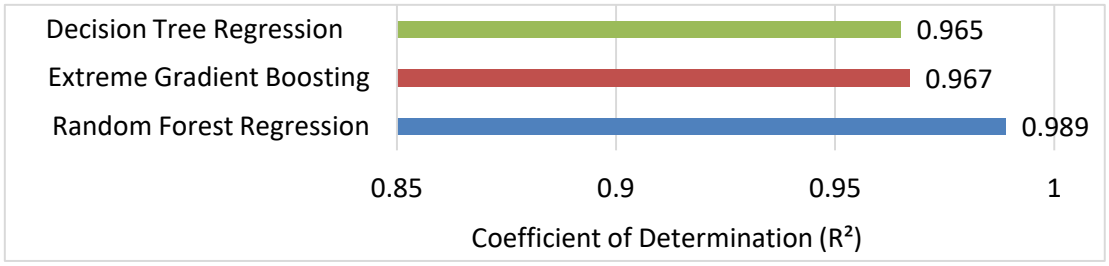

Figure 2. *Comparison of algorithms.*

Figure 3 presents the relation between actual and predicted RUL values for the plastic injection molding machine coded as HEP3204. It shows the effectiveness of the random forest model as an ensemble learning algorithm. Therefore, this model can be successfully used to predict the remaining useful life of the plastic injection molding machine in the future.

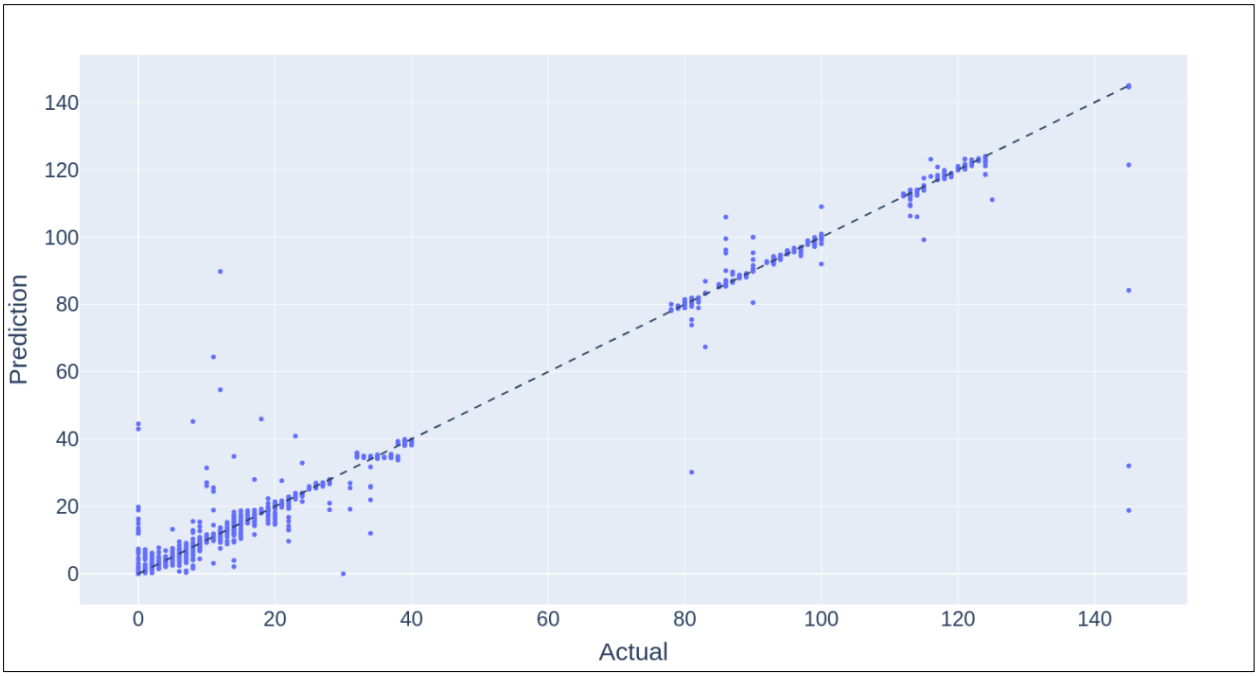

Figure 3. *Actual vs predicted RUL values.*

5. Conclusion and Future Work

In this study, we performed regression analysis for plastic injection molding machines based on the sensor values. Our goal was to estimate the remaining useful life of the machines with high accuracy. A pipeline of several data processing techniques was performed before machine learning algorithms were applied. We studied with the most prevalent regression algorithms, and based on the performance metrics, the Random Forest Regressor was the best model, achieving 0.989 in terms of R2, while XGBoost and Decision Tree Regression scored 0.967 and 0.965, respectively.

The findings of this study guided us to make a comprehensive analysis of the sensor data in terms of having a better insight into the contributions of each sensor to maintenance. In future work, we are planning to estimate the failure types of the machines based on the information we obtained from this research.

Declaration of Interest

The authors declare that there is no conflict of interest.

Acknowledgments

This study has been supported by the project numbered 9190028 carried out within the scope of the TUBITAK.

References

[1] A. Theissler, J. Perez-Velazquez, M. Kettelgerdes, and G. Elger, "Predictive maintenance enabled by machine learning: Use cases and challenges in the automotive industry," Reliability Engineering System Safety, vol. 215, pp. 1-21, 2021.

[2] D. Zhao and F. Liu, "Cross-condition and cross-platform remaining useful life estimation via adversarial-based domain adaptation," Scientific Reports, vol. 12, pp. 1-13, 2022.

[3] F. Yao, W. He, Y. Wu, F. Ding, and D. Meng, "Remaining useful life prediction of lithium-ion batteries using a hybrid model," Energy, vol. 248, pp. 1-13, 2022.

[4] H. Chen, Z. Zhan, P. Jiang, Y. Sun, L. Liao, X. Wan, Q. Du, X. Chen, H. Song, R. Zhu, Z. Shu, S. Li, and M. Pan, "Whole life cycle performance degradation test and RUL prediction research of fuel cell mea," Applied Energy, vol. 310, pp. 1-10, 2022.

[5] T. Böttjer, G. Rønsch, C. Gomes, D. Ramanujan, A. Iosifidis, and P.G. Larsen, "Data-driven identification of remaining useful life for plastic injection moulds," Lecture Notes in Mechanical Engineering, vol. 2022, pp. 431-439, 2022.

[6] C. Peng, Y. Chen, Q. Chen, Z. Tang, L. Li, and W. Gui, "A remaining useful life prognosis of turbofan engine using temporal and spatial feature fusion," Sensors, vol. 21, no. 2, pp. 1-20, 2021.

[7] S. Falconer, E. Nordgard-Hansen, and G. Grasmo, "Remaining useful life estimation of HMPE rope during CBOS testing through machine learning," Ocean Engineering, vol. 238, pp. 1-12, 2021.

[8] J.-Y. Wu, M. Wu, Z. Chen, X.-L. Li, and R. Yan, "Degradation aware remaining useful life prediction with LSTM autoencoder," IEEE Transactions on Instrumentation and Measurement, vol. 70, pp. 1-10, 2021.

[9] M. Ragab, Z. Chen, M. Wu, C.-K. Kwoh, R. Yan, and X. Li, "Attention based sequence to sequence model for machine remaining useful life prediction," Neurocomputing, vol. 466, pp. 58-68, 2021.

[10] Z. Kang, C. Catal, and B. Tekinerdogan, "Remaining useful life (RUL) prediction of equipment in production lines using artificial neural networks," Sensors, vol. 21, no. 3, pp. 1-20, 2021.

[11] P. F. Orru, A. Zoccheddu, L. Sassu, C. Mattia, R. Cozza, and S. Arena, "Machine learning approach using MLP and SVM algorithms for the fault prediction of a centrifugal pump in the oil and gas industry," Sustainability, vol. 12, no. 11, pp. 1-15, 2020.

[12] A. Bala, I. Ismail, R. Ibrahim, S. M. Sait, and D. Oliva, "An improved grasshopper optimization algorithm based echo state network for predicting faults in airplane engines," IEEE Access, vol. 8, pp. 159773– 159789, 2020.

[13] M. Utah and J. Jung, "Fault state detection and remaining useful life prediction in ac powered solenoid operated valves based on traditional machine learning and deep neural networks," Nuclear Engineering and Technology, vol. 52, no. 9, pp. 1998–2008, 2020.

[14] H.-C. Trinh and Y.-K. Kwon, "A data-independent genetic algorithm framework for fault-type classification and remaining useful life prediction," Applied Sciences, vol. 10, no. 1, pp. 1-20, 2020.

[15] M. Calabrese, M. Cimmino, F. Fiume, M. Manfrin, L. Romeo, S. Ceccacci, M. Paolanti, G. Toscano, G. Ciandrini, A. Carrotta, M. Mengoni, E. Frontoni, and D. Kapetis, "Sophia: An event-based iot and machine learning architecture for predictive maintenance in industry 4.0," Information, vol. 11, no. 4, pp. 1-17, 2020.

[16] Y. Chen, T. Zhang, W. Zhao, Z. Luo, and H. Lin, "Rotating machinery fault diagnosis based on improved multiscale amplitude-aware permutation entropy and multiclass relevance vector machine," Sensors, vol. 19, no. 20, pp. 1-26, 2019.

Journal of Artificial Intelligence and Data Science (JAIDA)
e-ISSN: 2791-8335
https://dergipark.org.tr/pub/jaida

Vol. 2, No. 1, pp. 16-23, 2022
Research Article

Improving the Design of Blade for Horizontal Axis Wind Turbine with QBlade Software

Prasun BHATTACHARJEE [1,*], Rabin K. JANA [2], Somenath BHATTACHARYA [3]

[1] Jadavpur University, Faculty of Engineering and Technology, Department of Mechanical Engineering, India
[2] Indian Institute of Management Raipur, Operations & Quantitative Methods Area, India
[3] Jadavpur University, Faculty of Engineering and Technology, Department of Mechanical Engineering, India

Abstract
As climate change is instigating massive human distress globally, several nations have agreed to minimize the release of greenhouse gases through the effective use of renewable energy resources like wind power through the Paris treaty of 2015 and COP-26 organized in Glasgow, Scotland. The blade is an important part of a wind turbine and its design impacts the efficiency of a wind farm immensely. In this paper, the design optimization of an NREL 5 MW horizontal axis wind turbine has been attempted with QBlade software. The optimized blade design validates improved co-efficient of power and developed stress profile.
Keywords: Blade; Horizontal Axis; NREL; QBlade Software; Wind Turbine.

1. Introduction

Because of the unreliable supply and detrimental effect of hydrocarbon-based fuels, renewable power generation techniques can support electricity generation businesses to generate power with minimal carbon footprint [1]. Wind energy is a competent renewable power generation resource and is assisting countries to produce electricity cost-effectively [2] [3].

Several kinds of research have been aimed at boosting the efficiency of wind power generation systems [4] - [16]. Researchers looked for important features of controlling and upkeep Wind Turbines (WTs). Nearly 0.28 annual breakdowns have been estimated for the blade tip of WT [17]. The breakdown proportions of German and Danish WTs applying the Windstats consistency details and power-law technique [18]. It has been detected that the collapse frequency for German WTs was to some extent more and was expected to fall to the identical magnitude of the malfunction proportions of Danish WTs after 7 years. A three-dimensional finite element prototype for fatigue crash of a completely composite-formed WT airfoil blade has been explored [19]. Because of the arbitrariness of the air flow form, a stochastic procedure had been betrothed to plan a software scheme for emulating the current of air with randomness on the WT blade, and afterward, each load case was associated with the conforming Weibull distribution.

In a study published in 2019, a software simulation has been undertaken for a small WT (less than 1 kW) rotor blade using the Blade Element Method (BEM) for maximizing the lift and drag coefficient ratio along with the power factor [20].

The present paper aims to increase the power co-efficient and the developed stress characteristics using the QBlade software for a 5 MW WT.

2. Problem Design

The current research has been performed for a horizontal axis WT. The power co-efficient of a WT can be calculated as per Eq. (1) [20].

$$C_p = \frac{P_{actual}}{P_{wind}} \tag{1}$$

where P_{actual} denotes the actual generated electrical power and P_{wind} signifies the available power flowing through the wind at a certain speed.

The process of WT design employing the QBlade software can be described as follows.

a) Design of the WT blade.
b) Modeling of the WT rotor,
c) Simulation of the entire WT.

In this current work, a National Renewable Energy Laboratory (NREL) 5 MW WT has been deemed. At first, the airfoil has been designed for a WT blade of 43.05 m.

The WT blade for standard NREL 5 MW WT has been shown in Fig. 1.

*Corresponding author e-mail address: prasunbhatta@gmail.com

Received: 28/04/2022; Accepted: 11/05/2022

Figure 1. *Standard NREL 5 MW WT Blade*

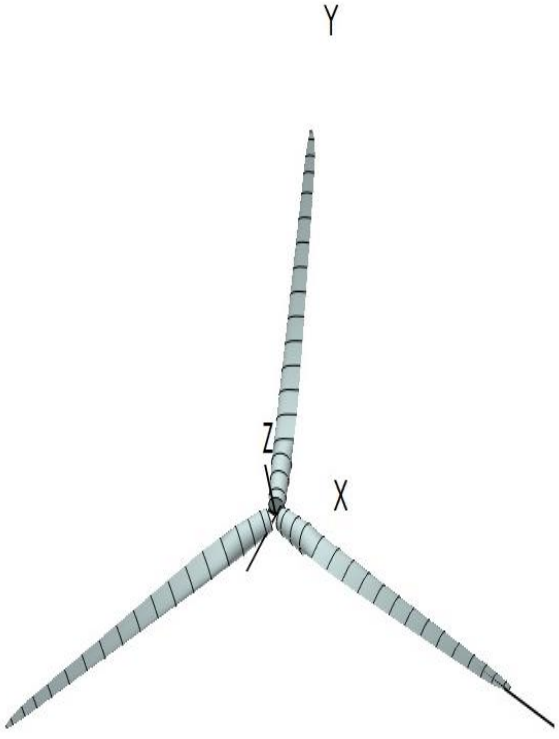

Figure 2. *Rotor View of Standard NREL 5 MW WT Blade*

Table 1. *Standard NREL 5 MW WT Blade Data*

Position (m)	Chord (m)	Twist	Foil
0	3.2	13.08	Circular Foil 0.5
1.36	3.54	13.08	Circular Foil 0.5
4.1	3.85	13.08	Circular Foil 0.5
6.83	4.67	13.08	Circular Foil 0.35
10.25	4.55	13.08	DU99W405LM
14.35	4.652	11.48	DU99W350LM
18.45	4.458	10.16	DU99W350LM
22.55	4.249	9.011	DU97W300LM
26.65	4.007	7.795	DU91W225LM
30.75	3.748	6.544	DU91W225LM
34.85	3.502	5.361	DU93W210LM
38.95	3.256	4.188	DU93W210LM
43.05	3.01	3.125	NACA64618

The simulated wind field with a mean airspeed of 13 m/s has been shown in Fig. 3.

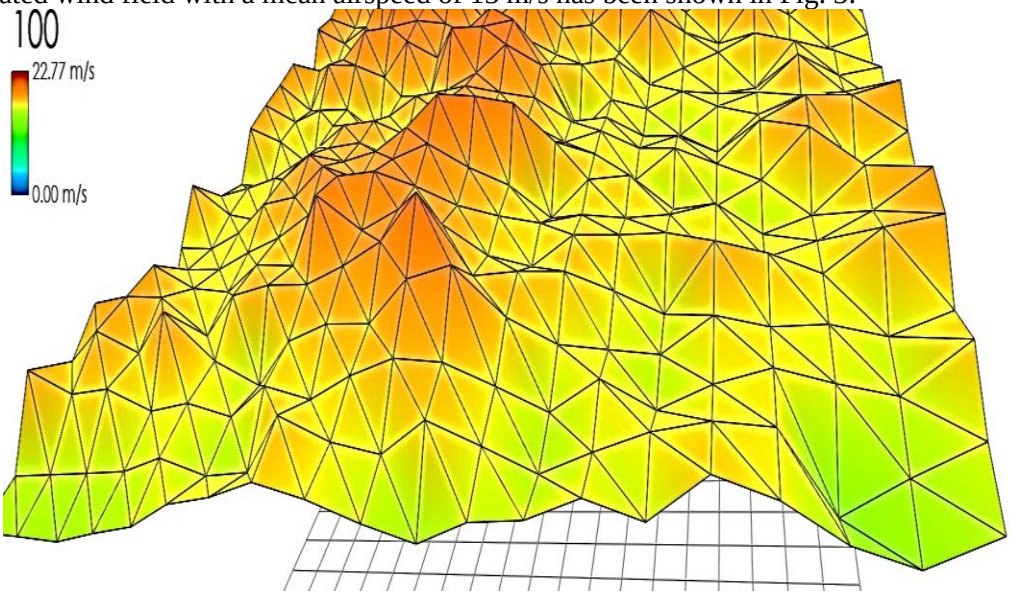

Figure 3. *Considered Wind Field*

The power simulation of standard NREL 5 MW WT has been shown in Fig. 4.

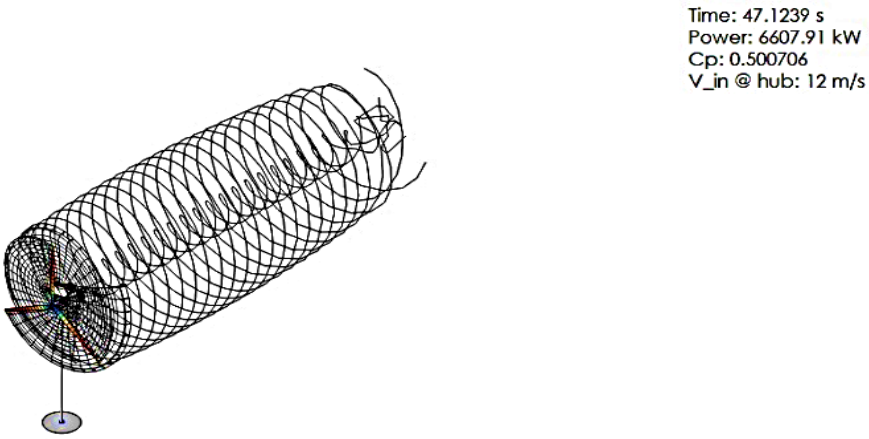

Figure 4. *Power Simulation Using Standard NREL 5 MW WT*

The loading condition on the WT blade has been presented in Table 2.

Table 2. *Loading Condition on the WT Blade*

Radial Position (m)	Normal Loading (N)	Tangential Loading(N)
0	4.65125	-4.31069
1.36	22.3584	-22.2077
4.1	43.0771	-62.938
6.83	64.9657	-102.651
10.25	366.223	53.4711
14.35	480.349	81.7205
18.45	474.401	53.9021
22.55	611.256	57.682
26.65	945.007	77.0227
30.75	1341.61	81.3494
34.85	1825.48	69.0401
38.95	2202.58	54.3237
43.05	2483.5	48.0438

3. Results and Discussion

The stress profile generated for the standard NREL 5 MW WT rotor blade using the loading condition of Table 2 has been shown in Fig. 5.

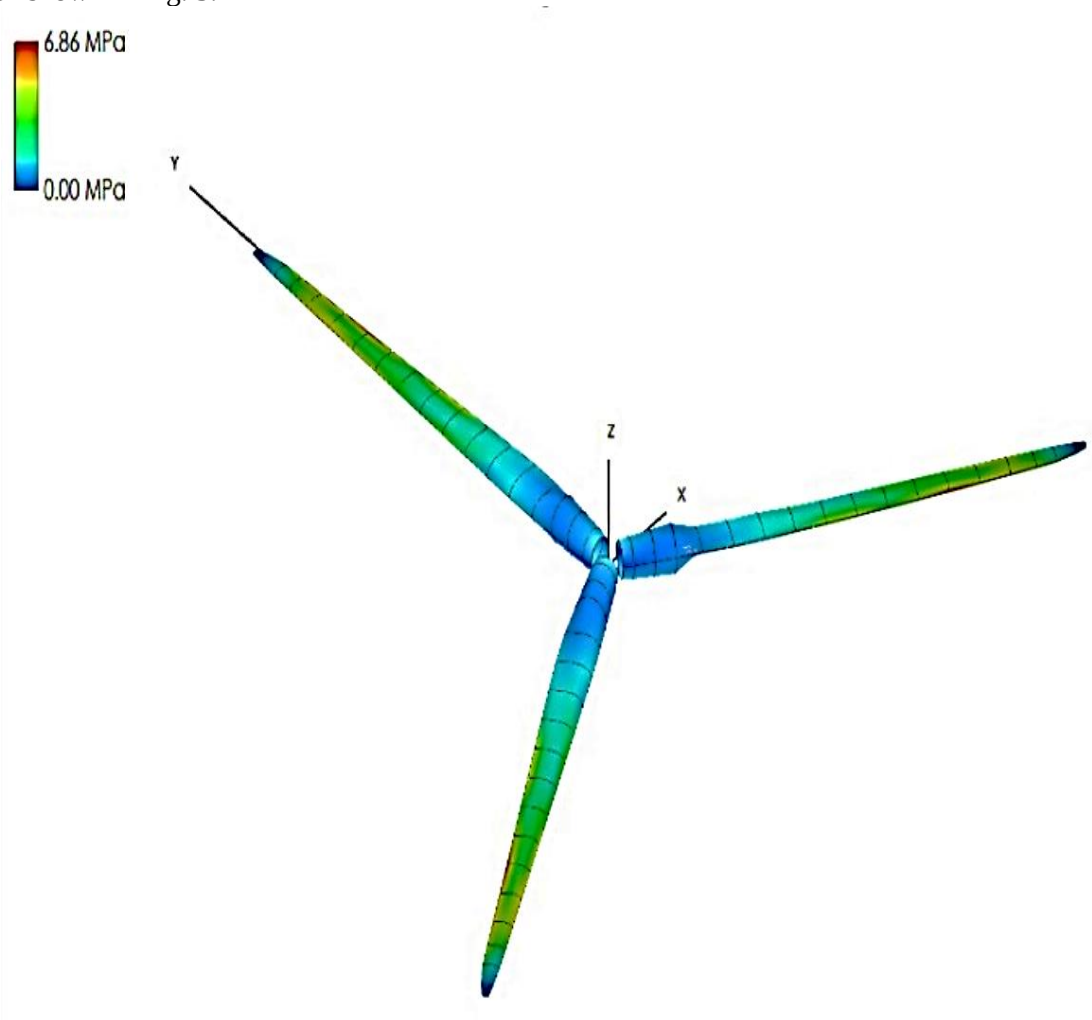

Figure 5. *Stress Profile of Standard NREL 5 MW WT with BEM*

Table 3. *Optimized NREL 5 MW WT Blade Data*

Position (m)	Chord (m)	Twist	Foil
0	3.2	13.08	Circular Foil 0.5
1.36	3.54	13.08	Circular Foil 0.5
4.1	3.85	13.08	Circular Foil 0.5
6.83	4.167	13.08	Circular Foil 0.35
10.25	10.4399	13.08	DU99W405LM
14.35	6.44813	11.48	DU99W350LM
18.45	6.69132	10.16	DU99W350LM
22.55	6.4402	9.011	DU97W300LM
26.65	5.33015	7.795	DU91W225LM
30.75	4.8217	6.544	DU91W225LM
34.85	4.10463	5.361	DU93W210LM
38.95	3.61205	4.188	DU93W210LM
43.05	3.4957	3.125	NACA64618

The optimized NREL 5 MW WT has been presented in Figs. 6 and 7.

Figure 6. *Optimized NREL 5 MW WT Blade*

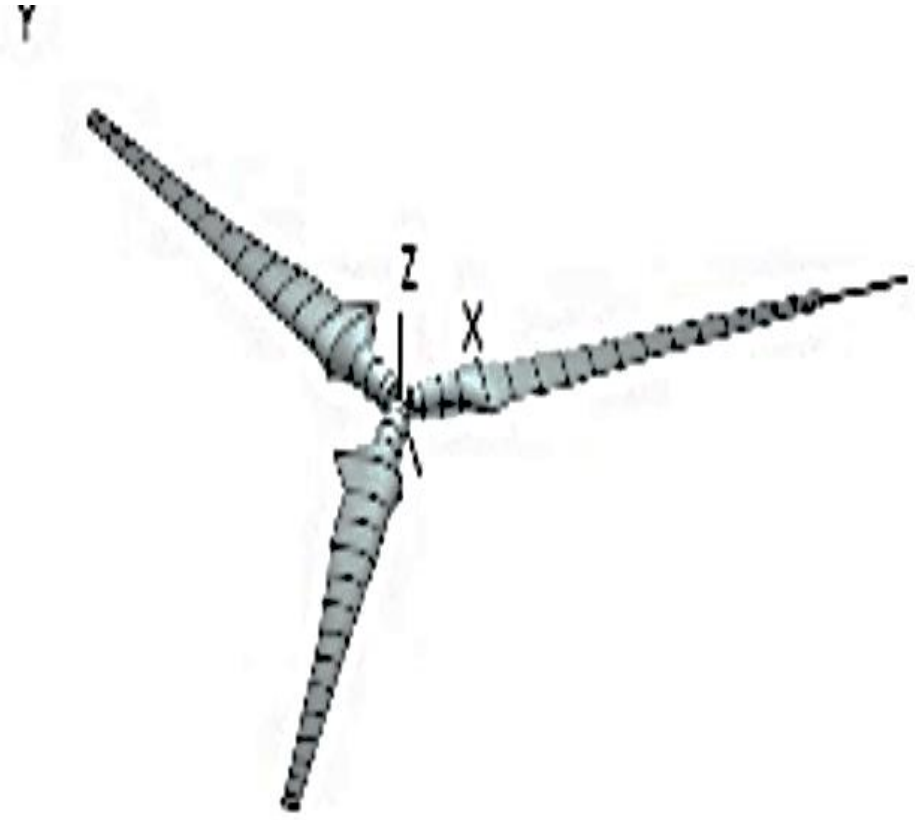

Figure 7. *Rotor View of the Optimized NREL 5 MW WT*

The simulated power co-efficient and BEM stress analysis has been shown in Figs. 8 and 9 respectively.

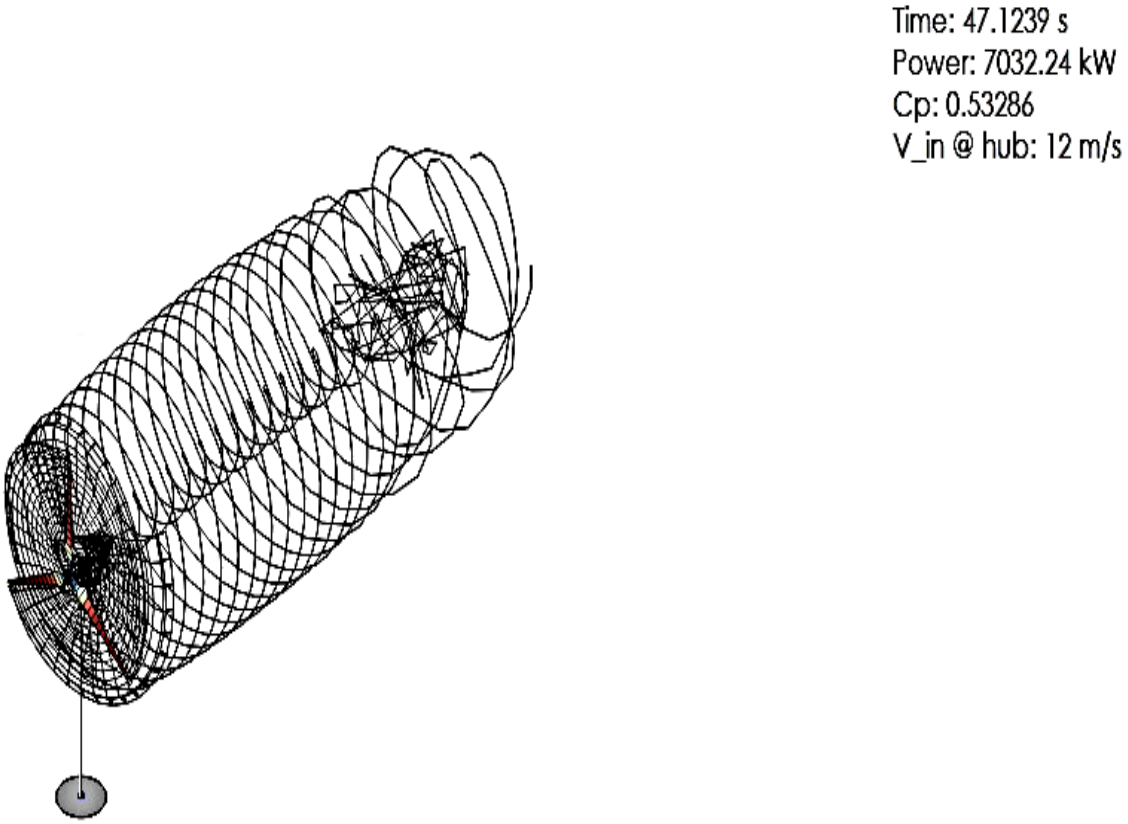

Figure 8. *Power Simulation of the Optimized NREL 5 MW WT*

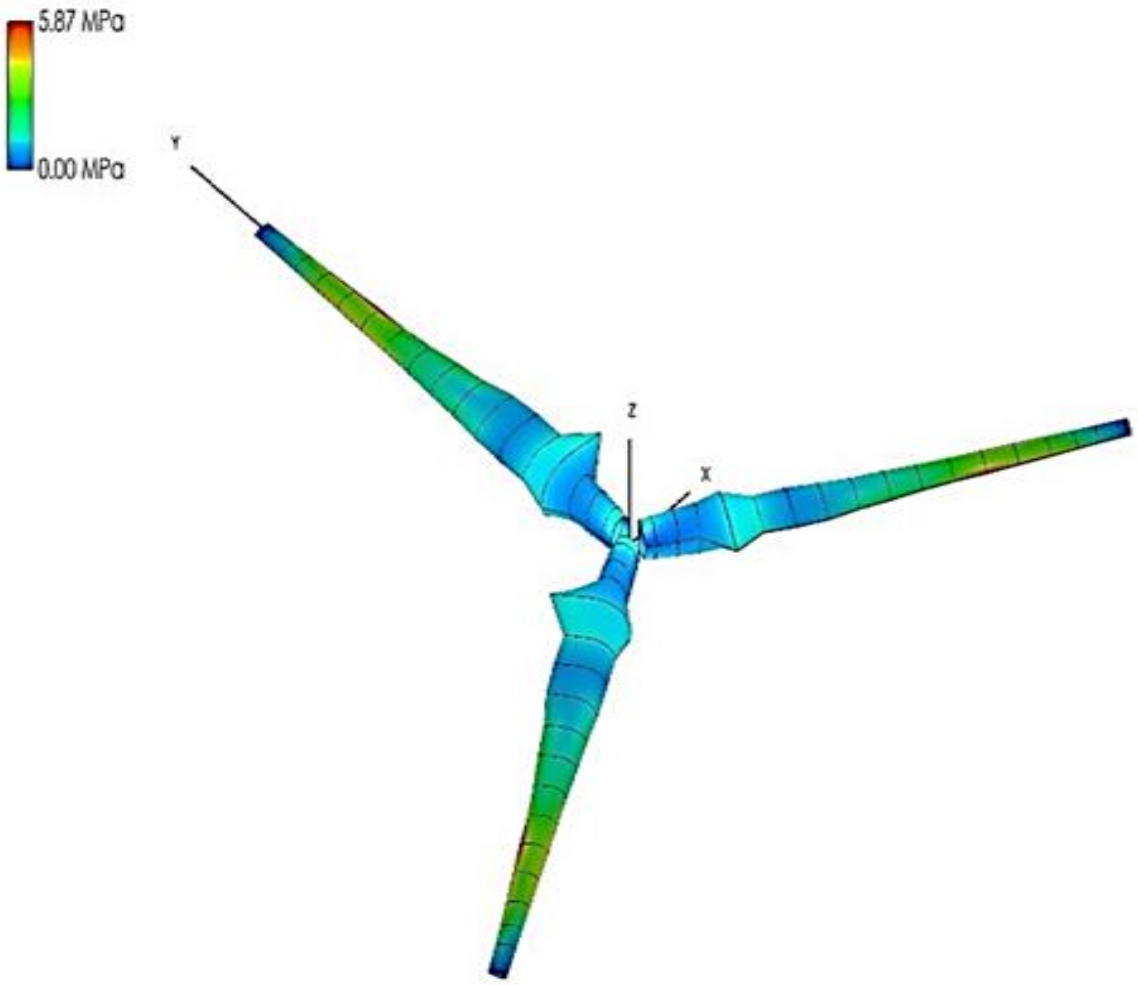

Figure 9. *Stress Profile of Optimized NREL 5 MW WT with BEM*

The power co-efficient and maximum generated stress for both the blade patterns have been presented in Table 4.

Table 4. *Comparative Analysis of Blade Profiles*

Blade Profile	**Power Co-efficient (C_p)**	**Maximum Developed Stress (σ_{max})**
Non-Optimized Standard NREL 5MW WT Rotor Blade	0.500706	6.86 MPa
Optimized NREL 5MW WT Rotor Blade	0.53286	5.87 MPa

The analysis validates the superiority of the optimized blade profile over the non-optimized standard NREL 5 MW WT rotor blade for presenting higher power co-efficient and lower maximum developed stress.

4. Conclusion

Wind power is being utilized transnationally for curbing the carbon footprint of the electricity generation sector. WT rotor blade design is an influential factor in optimizing the wind power generation system performance. In this paper, the design of the NREL 5 MW WT rotor blade has been enhanced to increase the power co-efficient and curtail the developed stress profile. This research can initiate novel prospects for wind power generation design improvement procedures.

Declaration of Interest

The authors declare that there is no conflict of interest.

Acknowledgements

The first author acknowledges the economic support of the TEQIP section of Jadavpur University for sustaining the present study.

References

[1] B. Obama, "The irreversible momentum of clean energy," Science, vol. 355, no. 6321, pp. 126-129, 2017.

[2] J. Cousse, R. Wüstenhagen and N. Schneider, "Mixed feelings on wind energy: Affective imagery and local concern driving social acceptance in Switzerland," Energy Research & Social Science, vol. 70, p. 101676, December 2020.

[3] R. Sitharthan, J. N. Swaminathan and T. Parthasarathy, "Exploration of Wind Energy in India: A Short Review," in 2018 National Power Engineering Conference (NPEC), 2018.

[4] P. Bhattacharjee, R. K. Jana and S. Bhattacharya, "A Comparative Analysis of Genetic Algorithm and Moth Flame Optimization Algorithm for Multi-Criteria Design Optimization of Wind Turbine Generator Bearing," ADBU Journal of Engineering Technology, vol. 10, 2021.

[5] P. Bhattacharjee, R. K. Jana and S. Bhattacharya, "A Comparative Study of Dynamic Approaches for Allocating Crossover and Mutation Ratios for Genetic Algorithm-based Optimization of Wind Power Generation Cost in Jafrabad Region in India," in Proceedings of International Conference on “Recent Advancements in Science, Engineering & Technology, and Management", Jaipur, India, 2021.

[6] P. Bhattacharjee, R. K. Jana and S. Bhattacharya, "A Relative Analysis of Genetic Algorithm and Binary Particle Swarm Optimization for Finding the Optimal Cost of Wind Power Generation in Tirumala Area of India," ITM Web of Conferences, p. 03016, 2021.

[7] P. Bhattacharjee, R. K. Jana and S. Bhattacharya, "A Relative Assessment of Genetic Algorithm and Binary Particle Swarm Optimization Algorithm for Maximizing the Annual Profit of an Indian Offshore Wind Farm," in Second International Conference on Applied Engineering and Natural Sciences, Konya, Turkey, 2022.

[8] P. Bhattacharjee, R. K. Jana and S. Bhattacharya, "Amplifying the Financial Sustainability of a Wind Farm near the Coast of Gujarat with an Augmented Genetic Algorithm," in International Symposium on Information & Communication Technology 2022, Greater Noida, India, 2022.

[9] P. Bhattacharjee, R. K. Jana and S. Bhattacharya, "An Enhanced Genetic Algorithm for Annual Profit Maximization of Wind Farm," Journal of Information Systems & Operations Management, vol. 15, no. 2, 2021.

[10] P. Bhattacharjee, R. K. Jana and S. Bhattacharya, "An Enriched Genetic Algorithm for Expanding the Yearly Profit of Wind Farm," in Second International Symposium on Intelligence Design (ISID 2022), Tokyo, Japan, 2022.

[11] P. Bhattacharjee, R. K. Jana and S. Bhattacharya, "Augmenting the Yearly Profit of Wind Farm," in The 14th Regional Conference on Electrical and Electronics Engineering of Chulalongkorn University, Bangkok, Thailand, 2022.

[12] P. Bhattacharjee, R. K. Jana and S. Bhattacharya, "An Improved Genetic Algorithm for Yearly Profit Maximization of Wind Power Generation System," in The 31st ACM SIGDA University Demonstration, New York, USA, 2021.

[13] P. Bhattacharjee, R. K. Jana and S. Bhattacharya, "Maximizing the Yearly Profit of an Indian Nearshore Wind Farm," in First International Conference on Applied Engineering and Natural Sciences, Konya, Turkey, 2021.

[14] P. Bhattacharjee, R. K. Jana and S. Bhattacharya, "Multi-Objective Design Optimization of Wind Turbine Blade Bearing," Invertis Journal of Science & Technology, vol. 14, no. 3, pp. 114-121, 2021.

[15] P. Bhattacharjee, R. K. Jana and S. Bhattacharya, "Optimizing Offshore Wind Power Generation Cost in India," in Third New England Chapter of AIS (NEAIS) Conference, Boston, Massachusetts, 2021.

[16] P. Bhattacharjee, R. K. Jana and S. Bhattacharya, "Realizing The Optimal Wind Power Generation Cost in Kayathar Region of India," in International Conference on Information, Communication and Multimedia Technology - 2021 (ICICMT - 2021), Madurai, 2021.

[17] G. Van Bussel and A. Henderson, "State of the Art and Technology Trends for Offshore Wind Energy: Operation and Maintenance Issues," in In Proceedings of offshore wind energy special topic conference, Brussels, Belgium, 2001.

[18] P. J. Tavner, J. Xiang and F. Spinato, "Improving the reliablity of wind turbine generation and its impact on overall distribution network reliablity," in 18th International Conference on Electricity Distribution (CIRED 2005), 2005.

[19] M. M. Shokrieh and R. Rafiee, "Simulation of fatigue failure in a full composite wind turbine blade," Composite Structures, vol. 74, no. 3, pp. 332-342, 2006.

[20] M. Alaskari, O. Abdullah and M. H. Majeed, "Analysis of wind turbine using QBlade software," in IOP conference series: materials science and engineering, 2019.

Journal of Artificial Intelligence and Data Science (JAIDA)
e-ISSN: 2791-8335
https://dergipark.org.tr/pub/jaida

Vol. 2, No. 1, pp. 24-30, 2022
Review Article

Arabic Sentiment Analysis: Reviews of the Effective Used Algorithms

İnas CUMAOĞLU [1*], Vedat TÜMEN [2], Yüksel ÇELIK [1]

[1] Karabük University, Engineering Faculty, Department of Computer Engineering, Turkey
[2] Bitlis Eren University, Engineering Faculty, Department of Computer Engineering, Turkey

Abstract
Sentiment analysis (SA) attracted many researchers due to its success in many areas such as marketing, health, and politics. It is a science of artificial intelligence (AI) and natural language processing (NLP), which aims to study people's thoughts, attitudes, and aspirations on a subject. SA is based on textual data obtained from internet sites such as electronic stores, flight and hotel reservation sites, and social media sites like Twitter and Facebook. However, the problem with that data is that it is unstructured and unorganized. The researchers had to work on organizing it using NLP tools to deal with it and analyze the feelings extracted from this data. Due to the grammatical and morphological complexity of the Arabic language and the lack of an Arabic corpus, it is still in the early phases of processing Arabic texts compared to English texts. As a result, in this research, we examined the most recent literature and scientific studies on Arabic sentiment analysis (ASA) to identify the most important algorithms that have demonstrated their quality and usefulness in this sector. We observed the researchers' interest in the use of deep learning algorithms (DL), which demonstrated their efficacy in this field and the employment of a variety of text extraction approaches, the most prominent of which were the TF-IDF CBOW and Skip-gram.
Keywords: Arabic sentiment analysis; data mining, deep learning; NLP; social media.

1. Introduction

Sentiment analysis (SA) is one of the most important and most attractive sciences for researchers. Furthermore, it is one of the applications of natural language processing (NLP), which was born from three sciences, namely, human linguistics, computer science, and artificial intelligence [1]. Some researchers also call it data mining. The importance of this science lies in the ability to apply it to many areas of life, such as politics, health, marketing, finance, and others.

In marketing, it has been proven that SA should be applied to giant companies and institutions that wish to enhance their revenues and customer base by knowing the opinion of customers about their products and services. So the process of knowing the customer's opinion and reading his thoughts and aspirations is the process of SA. [2].

SA participated in political fields and predicted the victory of a candidate by analyzing the feelings of the people and the public [3]. In the financial markets, automated applications based on sentiment analysis have proven to be more efficient than human analysts[4]. Although sentiment analysis has made tangible progress in English texts, it is still in the process of being challenged and discovered in Arabic texts. The Arabic language is complex and rich in words, synonyms, and expressions, which made addressing it a challenge and a science racing to fill its gaps [5]. Moreover, because social media was overcrowded with Arab subscribers and users, the Arabic data became huge, large, and diverse. So researchers needed to collect this unstructured data by reorganizing it and using it in natural language processing and sentiment analysis in SA.

2. Sentiment Analysis

In recent years, social networking sites have increased and become more and more popular, which has led to the presence of extensive and big data in different languages, including the Arabic language, which has a diversity and multiplicity of dialects. Indeed, this data is helpful, but it is random and unorganized.

So, NLP and SA came to process these data, contribute to organizing it, and benefit from knowing opinions, feelings, and trends in various economic and political aspects. Such as improving product quality, predicting a candidate's election victory, forecasting stocks and the stock market, and various other applications.

SA is one of the NLP applications, as shown in Figure 1, concerned with studying people's attitudes, thoughts, and tendencies through comments, posts, reviews, or tweets that they share on websites and social media. Thus texts are divided into categories and classes using artificial intelligence AI, ML, and DL algorithms.

*Corresponding author e-mail address: inascu90@gmail.com

Received: 08/05/2022; Accepted: 22/06/2022

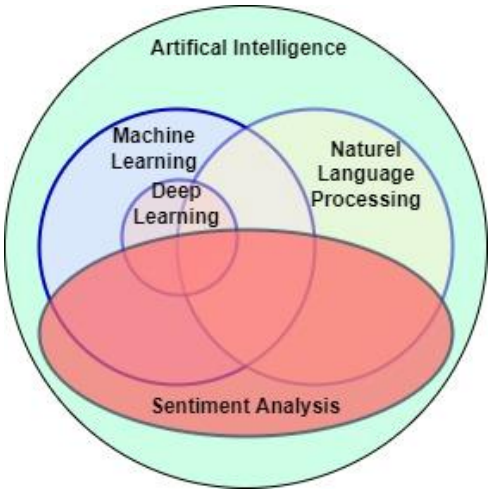

Figure 1. *Artificial Intelligence, Machine Learning, Deep Learning, Natural Language Processing, and Sentiment Analysis*

SA is also divided into three levels, as shown in Figure 2, where the document level deals with the feelings in the file as a whole without dividing it into sentences. In contrast, the sentence level deals with the feelings in each sentence separately, after making sure that it is a subject sentence containing feelings and not an object sentence without feelings and talking about facts. The aspect-based sentiment analysis level (ABSA) evaluates the feeling after dividing the content into several aspects and then discovers the feeling or polarity in each sentence after defining the aspect [6].

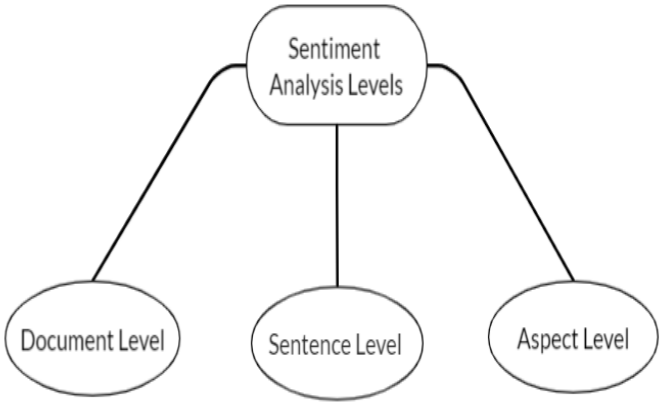

Figure 2. *Sentiment Analysis Levels*

2.1. Arabic sentiment analysis challenges

The Arabic language is a morphologically complex language with a plurality of dialects. The pioneers of social communication prefer to express their opinions using the various dialects of their countries. That has led to difficulty addressing the Arabic language because each dialect contains expressions that differ from country to country. For example, the word for a man in the Levant is "rajul"; In Sudan; it is "Zol " Also, the Arabic language does not contain uppercase or lowercase letters; instead, the Arabic letters differ in how they are written according to their position in the word. In addition, it is written from right to left, in contrast to writing the Latin letters. In addition, the diacritics of Arabic letters and prefixes and suffixes constitute an obstacle in the treatment of the Arabic language. Also, the lack of Arab corpus is one of the biggest challenges facing researchers [7]

3. Literature Review

In this section, we will introduce the recent literature with the used algorithms and the results of the experiments:

Alharbi and Qamar [8] suggested analyzing customers' feelings who visit cafes and restaurants in the Qassim region by conducting an opinion survey via Microsoft Form to improve the Saudi economy. A dataset with a size

of 1785 reviews was created, and then it was reduced after filtering and pre-processing to 1,507 reviews in Arabic. Using five machine learning algorithms (KNN, NB, LR, AVM, and RF) after feature extraction by Term Frequency Inverse Document Frequency (TF-IDF), they could reach 89% accuracy by SVM, 93% F-measure by RF, and 92 % recall also by SVM.

In order to classify the text into two categories, positive and negative, Sayed et al. [9] created a dataset from the reviews of hotel customers on the Booking.com website. Thus, an Arabic corpus was created in the colloquial dialect and MSA with the name (RSAC), an abbreviation for Review Sentiment Analysis Corpus, and includes 6318 reviews divided into 3354 positive and 2964 negative. They used TF_IDF with unigrams after the initial processing, including stop words and non-Arabic letter removal. Then trained the model using nine algorithms of machine learning, six traditional (LR, SVM, KNN, NB, DT, RF) and three new ones not used previously in text classification (Gradient Boosting(GB), Ridge classifier (RC), Multilayer Perception (MCL)). At last, they tested the performance many times: one without applying any pre-processing and one more with applying stop words removal, another with the effect of stemming, and one with utilizing all pre-processing techniques according to accuracy, recall, precision, and F1- score and found that RC was the best one with 95% accuracy.

Abuuznien et al. [10] suggested using machine learning algorithms to know the Sudanese people's opinion of the ride-sharing service. So they collected Arabic corps from Twitter in their Sudanese dialect. The dataset consisted of 768 positive, 841 negatives, and 507 neutral tweets. It extracted 686 stop words in the Sudanese dialect added to the MSA stop word set. Then the pre-possessing phase started, and they used TF_IDF with n-gram to convert words into a vector, and in the classification phase, they used KNN, NB, and SVM to divide tweets into positive, negative, or neutral. They tested the efficiency of the models after following several techniques from Pre-Processing by measuring accuracy and F1 score, and they noticed that SVM presented a higher efficiency than the other two classifiers, with an accuracy of 95% after applying stemming as Pre-Processing.

Al-Tamimi et al. [11] collected data from comments on YouTube videos using YouTube API to analyze sentiments from the Arabic text. They also developed a windows application to help them annotate the data, so they built the dataset based on positive, negative, and neutral comments and the relevance of the comment to the content of the video. Then they started with the pre-processing step by removing comments written in a non-Arabic language and removing the diacritics, and using unigram and bigram with TF-IDF to create the input vector. Using KNN, Bernoulli NB, and SVM with RBF (Radial Bases Function), the data were classified in various forms (balanced, unbalanced, raw, after normalization, with positive and negative classes, and the dataset with three classes positive, negative and neutral). Consequently, they found that SVM with RBF achieved the best result in terms of F-Measure when they applied it to the unbalanced two-class dataset and after the normalization process.

In a case study of the opinions and sentiments of Qassim University students, Alassaf et al. [12] suggested the use of ABSA. They started collecting data related to Al Qassim University from Twitter via Twitter API, and it was 8,234 tweets in size. It was reduced to 7,934 after deleting the tweets whose classification differed by annotators and after the Pre-Processing phase. In this work, they chose nine aspects for analysis in aspect detection, including the educational Aspect, the activities, and the environment. In addition, they defined the polarity of opinion in the Aspect- opinion classification task, which they suggested calling the classes negative or non-negative polarity. The non-negative category included a few positive tweets with neutral tweets. They used SVM with ANOVA to determine features and determine the affiliation of the tweet to one of the nine aspects. They also used F- score 20% _ Reg technique to reduce features to be 7,361 after it was 161,396 (4.5% decreased). Then they utilized SVM and cross-validation with ten fold to measure the model's efficiency.

Omara et al. integrated 13 available Arabic datasets in Modern Standard Arabic (MSA) and Dialectal from various domains, including book, film, restaurant, hotel, product, and tweet reviews. There are 92123 items in the new dataset, with 71112 positive and 21011 positive samples. Pre-processing was used to increase the quality of the results. For Arabic sentiment analysis (ASA), they proposed employing three deep convolutional neural networks (CNNs). Moreover, to extract features, they used character level with CNN. Hence, they tested the model on both pre-processed and raw data sets and compared it to 8 standard machine learning classifiers. After evaluation, they noticed that the suggested model outperforms machine learning classifiers by about 7% [13].

Abdelli et al. compared the performance of machine learning and deep learning in classifying Arabic texts in MSA and colloquial Algerian dialect using the SVM algorithm, which is one of the supervised machine learning algorithms, with the TFIDF technique for feature extraction. In contrast, they used LSTM, one of the DL algorithms with Continuous Bag of Words (CBOW) for Word Embedding. Two data sets were created to achieve the work. One for sentiment analysis included data collected by the author from Facebook using Facebook API, then categorized into positive and negative comments and added to three pre-existing data sets made by other

researchers. After filtering the data and deleting the duplicated ones, the final dataset contained 49,864 elements, divided equally into positive and negative sentences. At the same time, the second dataset contained 1.4 gigabytes of Arabic Corpus merging from a pre-existing Arabic Corpus to be used in CBOW training. SVM outperformed LSTM in accuracy in this work, reaching 86% [14].

Ombabi et al. [15] combined five re-published data sets in many topics written in Arabic to be 15.100 reviews in total, divided into positive and negative classes equally. The authors proposed a Deep CNN-LSTM Arabic-SA model that works as follows:

After re-processing and normalization phase, they used FastText (Skip-gram and CBOW) as word embedding methods to be the input of CNN to extract features, then used fully connected LSTMs at last used SVM for classification and prediction. A confusion matrix measured the performance, and the accuracy was achieved at 90.75%. It is worth noting that the authors tested the efficiency of the proposed model using other classifiers (NB and KNN), but SVM was the classifier with the highest efficiency.

To ASA, Khalid Bolbol and Maghari applied KNN, LR, and DT classifiers on four pre-existing data sets in different sizes in Arabic, where ASTD's size was 399 KB, AJGT 160KB, ASTC 5.5 MB, and Arabic 100K Reviews 35.4 MB. Consequently, they pre-processed the data and extracted features by CBOW and TF-IDF techniques. The experiment showed that LR was the best accuracy [16].

The authors collected the dataset from Twitter about Covered-19 to classıfy ıt ınto posıtıve when there is fear or anxiety and negative when there is not a feeling of fear. They had balanced the collected dataset from social media for COVID-19 with pre-trained models CC.AR.300 and Arabic news. Then the authors pre-processed the dataset, and for feature extraction, using Word2Vec. The dataset was imbalanced, so they used SMOTENN on the training data to balance it. They utilized the SMOTE technique by synthesizing new minority samples and then merging or removing some samples from both classes (minority and majority); however, it uses k=3 nearest neighbors to locate samples in a misclassified dataset. They used nuSVC, LSVC, LRSV, SGD, and BNB. When applying word2vector with SMOTEEN on CC.AR.300 and in Arabic News, the performance was better than applying word embedding without SMOTEEN [17].

In this paper, the authors relied on Aspect Based Sentiment Analysis to analyze the sentiments of Arab customers in Saudi Arabia about the services of three Saudi telecom companies. Alshammari and Almansour collected 6182 tweets and then filtered and pre-processed them into 1096 tweets related to customer opinions about telecom companies. This dataset is divided into 80% for training and 20% for testing after being labeled manually. To extract features, they use unigram and bigram, then TF-IDF. At last, for sentiment analysis, the author compared the performance of SVM, LR, and RF with deep learning algorithms. The experiment showed that LR with unigram gave higher performance compared with the performance of the SVM, RF with unigram and bigram, and with the performance of LR with bigram. In contrast, the efficiency of deep learning performance with word embedding is better than the performance of machine learning classifiers and deep learning with POS, with an accuracy of 81% [18].

Elfaik and Nfaoui suggested using AraVec (CBOW) with BiLSTM with the attention model to apply it to three Arabic data sets: ASTD, ArTwitter, and Main AHS. The experiment showed that the performance of the proposed model outperformed the performance of several other algorithms used in previous studies [19].

In this paper, The proposed model architecture is DeepASA (Deep learning for Arabic Sentiment Analysis) which consists of an Input Layer required to transform the input into numerical representation using word embedding (FastText and word2vector). On the other hand, the structure of the DeepASA model has three main layers (input layer, hidden layer, and output layer). The hidden layer has two main neural networks (LSTM & GRU). For the dataset, the model experimented with many datasets (LABR, RES, HTL, PROD, ARTwitter, ASTD). DeepASA trained and tested with these datasets after being balanced for classification. They combined 3-different machine learning classifiers, and SVM, GNB, and LR produced the highest accuracy. Result: DeepASA scored the highest accuracy when trained and tested with the HTL dataset, and accuracy reached 94.32% [20].

In the case of this paper, Dataset: Arabic book reviews contain 63,257 reviews collected from Goodreads with ratings positive reviews reaching 42,832 and negative are 8224, and this is the balanced version of the dataset. For word embedding layers in proposal mode, they use Glove for word representation and FastText. The Neural network architecture (Model) uses the RNN, LSTM, and FastText models. LSTM model has the highest accuracy with 89.82 compared with the CNN model [21].

They created two different data sets in the Sudanese dialectical. SudSenti2 dataset was collected from Facebook and YouTube posts with 2,027 positive comments and 1,973 negative comments. At the same time, SudSenti3 data set was collected from Twitter with 2,523 positive tweets and 2,639 negative ones. after pre-processing the data, they used TF-IDF and the AraVec (word embedding). They offered a Sentiment

Convolutional Model (SCM) with Mean Max Average (MMA) pooling layer. They applied it to both created data sets and two pre-existed datasets in MSA (HARD dataset) and Saudi dialects (SSD dataset). The proposed model SCM+MMA showed the highest accuracy compared with traditional ML algorithms and CNN, RNN, and LSTM+CNN. The accuracy when the model applied on SudSenti2(2 classes) was 92.75%,on SSD(2 classes) was 85.55%, on HARD (2 classes) was 90.01%, while on SudSenti3(3classes) was 84.39%.[22].

Table 1. *Basic information in the literature*

Reviewed Paper	Domain, Dataset	Language	Algorithms	Features	Accuracy
[8]	Twitter, Microsoft Form	Saudi dialect	KNN, NB, LR, AVM, RF	TF-IDF	89% by SVM
[9]	Reviews from the Booking.com website	MSA, DA	LR, SVM, KNN, NB,DT,RF, GB, RC, MCL	Unigram, TF-IDF	95% by RC
[10]	Twitter	Sudanese dialect	KNN, NB, SVM	N-gram, TF-IDF	95% by SVM
[11]	YouTube comments	MSA, DA	KNN, Bernoulli NB, SVM with RBF (Radial Bases Function)	N-gram, TF-IDF	88% F-measure by SVM - RBF
[12]	Twitter	Saudi dialect	SVM	ANOVA based on F values	98% F1 score
[13]	Multi-Domain Reviews merged from: TDS, ASTD, SemEval, Social Media Posts, OCA, LABAR, LARGE, Health Services	MSA, DA	CNNs, KNN, SVM ,LR, DT, RF, BernoulliNB, Multinomial NB	character level (CNN), TF-IDF, unigram, bigram	94% by CNNs with character level.
[14]	Facebook comments	MSA, Algerian dialect	SVM, LSTM	TF-IDF, CBOW	86% by SVM and TF-IDF
[15]	Multi-Domain reviews	MSA, DA	CNN–LSTM, SVM, NB, KNN	Skip-gram, CBOW, CNN	SVM with Skipgram 90.75%
[16]	Multi-Domain reviews	MSA, DA	KNN, LR, and DT	CBOW , TF-IDF	93% by LR
[17]	Twitter, CC.AR.300, Arabic. news	MSA, DA	RF, SGD, SVM, BNB, and LRCV	CBOW and skip-gram	98.55% by NuSVM in CC.AR.300, 97.67% by NuSVM in Arabic. news
[18]	Twitter	Saudi dialect	SVM, LR, RF, Deep learning	unigram , bigram , TF-IDF	78% LR with unigram, Deep learning with word embedding 81%
[19]	ASTD, ArTwitter and Main AHS	MSA, DA	AraVec (CBOW) + BiLSTM + attention, Gaussian NB (GNB), RF, Nu-support vector (NuSYC), Stochastic gradient descent (SGD), (LR)	CBOW	By AraVec + BiLSTM + attention in ASTD 73%, in ArTwitter 83%, and in Main AHS, 89%
[20]	Multi-Domain reviews	MSA, DA	DeepASA LSTM & GRU	FastText Word2vector Doc2vector	With HTL dataset acc 94.32%
[21]	Arabic book reviews	MSA, DA	LSTM&CNN	Glove FastText	LSTM Model 89.82
[22]	SudSenti2, SudSenti3, SSD, HARD	MSA, Saudi dialect, Sudanese dialect	SCM+MMA, CNN, RNN, and CNN+LSTM, LR, RF, NB, and SVM	Word imbedding, TF-IDF, CNN	SCM+MMA model on SudSenti2 92.75%, on SudSenti3 84.39%, On SSD 85.55%, and on HARD 90.01%.

4. Discussion

In most papers, SVM shows high efficiency and good accuracy. Also, using CNN to extract features could increase the model's effectiveness. We notice that most of the papers show the phase of extracting the features from input after the pre-processing, and modern methods like FastText and Golve improve the accuracy up to 92% in most of the papers. On the other hand, extracting features using the traditional method does not reach an

accuracy above 80%. For the proposal models trained and tested, the model LSTM &CNN with SVM classifier shows perfect results with an accuracy of 90.75%. However, the old model like KNN SVM, etc... does not reach high accuracy; most of the paper depends on traditional models to train that build on machine learning algorithms. Nevertheless, the model built on a deep learning algorithm shows the highest accuracy at 94.32 with the SVM classifier and Golve & FastText.

5. Conclusion

In this work, we presented a literature review of scientific papers in the field of ASA to help researchers know the best algorithms used in classification and in extracting features that have left a good impact in this field. In future work, we would like to use DL's algorithms to analyze Arab sentiments in Turkey.

Declaration of Interest

The authors declare that there is no conflict of interest.

References

[1] K. Jiang and X. Lu, "Natural Language Processing and Its Applications in Machine Translation: A Diachronic Review," *Proc. 2020 IEEE 3rd Int. Conf. Safe Prod. Informatiz. IICSPI 2020*, pp. 210–214, Nov. 2020, doi: 10.1109/IICSPI51290.2020.9332458.

[2] S. Al-Otaibi *et al.*, "Customer Satisfaction Measurement using Sentiment Analysis," *IJACSA) Int. J. Adv. Comput. Sci. Appl.*, vol. 9, no. 2, 2018, Accessed: Mar. 05, 2022. [Online]. Available: www.ijacsa.thesai.org.

[3] A. Das, K. S. Gunturi, A. Chandrasekhar, A. Padhi, and Q. Liu, "Automated Pipeline for Sentiment Analysis of Political Tweets," pp. 128–135, Jan. 2022, doi: 10.1109/ICDMW53433.2021.00022.

[4] K. Mishev, A. Gjorgjevikj, I. Vodenska, L. T. Chitkushev, and D. Trajanov, "Evaluation of Sentiment Analysis in Finance: From Lexicons to Transformers," *IEEE Access*, vol. 8, pp. 131662–131682, 2020, doi: 10.1109/ACCESS.2020.3009626.

[5] R. Duwairi and F. Abushaqra, "Syntactic- and morphology-based text augmentation framework for Arabic sentiment analysis," *PeerJ Comput. Sci.*, vol. 7, pp. 1–25, 2021, doi: 10.7717/PEERJ-CS.469/.

[6] S. V. Pandey and A. V. Deorankar, "A Study of Sentiment Analysis Task and It's Challenges," *Proc. 2019 3rd IEEE Int. Conf. Electr. Comput. Commun. Technol. ICECCT 2019*, Feb. 2019, doi: 10.1109/ICECCT.2019.8869160.

[7] Y. Zahidi, Y. E. L. Younoussi, and Y. Al-Amrani, "Arabic Sentiment Analysis Problems and Challenges," *Proc. - 10th Int. Conf. Virtual Campus, JICV 2020*, Dec. 2020, doi: 10.1109/JICV51605.2020.9375650.

[8] L. M. Alharbi and A. M. Qamar, "Arabic Sentiment Analysis of Eateries' Reviews: Qassim region Case study," *Proc. - 2021 IEEE 4th Natl. Comput. Coll. Conf. NCCC 2021*, Mar. 2021, doi: 10.1109/NCCC49330.2021.9428788.

[9] A. A. Sayed, E. Elgeldawi, A. M. Zaki, and A. R. Galal, "Sentiment Analysis for Arabic Reviews using Machine Learning Classification Algorithms," *Proc. 2020 Int. Conf. Innov. Trends Commun. Comput. Eng. ITCE 2020*, pp. 56–63, Feb. 2020, doi: 10.1109/ITCE48509.2020.9047822.

[10] S. Abuuznien, Z. Abdelmohsin, E. Abdu, and I. Amin, "Sentiment Analysis for Sudanese Arabic Dialect Using comparative Supervised Learning approach," *Proc. 2020 Int. Conf. Comput. Control. Electr. Electron. Eng. ICCCEEE 2020*, Feb. 2021, doi: 10.1109/ICCCEEE49695.2021.9429560.

[11] A. K. Al-Tamimi, A. Shatnawi, and E. Bani-Issa, "Arabic sentiment analysis of YouTube comments," *2017 IEEE Jordan Conf. Appl. Electr. Eng. Comput. Technol. AEECT 2017*, vol. 2018-January, pp. 1–6, Jul. 2017, doi: 10.1109/AEECT.2017.8257766.

[12] M. Alassaf and A. M. Qamar, "Aspect-Based Sentiment Analysis of Arabic Tweets in the Education Sector Using a Hybrid Feature Selection Method," *Proc. 2020 14th Int. Conf. Innov. Inf. Technol. IIT 2020*, pp. 178–185, Nov. 2020, doi: 10.1109/IIT50501.2020.9299026.

[13] E. Omara, M. Mosa, and N. Ismail, "Deep Convolutional Network for Arabic Sentiment Analysis," *2018 Proc. Japan-Africa Conf. Electron. Commun. Comput. JAC-ECC 2018*, pp. 155–159, Apr. 2019, doi: 10.1109/JEC-ECC.2018.8679558.

[14] A. Abdelli, F. Guerrouf, O. Tibermacine, and B. Abdelli, "Sentiment Analysis of Arabic Algerian Dialect Using a Supervised Method," *Proc. - 2019 Int. Conf. Intell. Syst. Adv. Comput. Sci. ISACS 2019*, Dec. 2019, doi: 10.1109/ISACS48493.2019.9068897.

[15] A. H. Ombabi, W. Ouarda, and A. M. Alimi, "Deep learning CNN–LSTM framework for Arabic sentiment analysis using textual information shared in social networks," *Soc. Netw. Anal. Min. 2020 101*, vol. 10, no. 1, pp. 1–13, Jul. 2020, doi: 10.1007/S13278-020-00668-1.

[16] N. Khalid Bolbol and A. Y. Maghari, "Sentiment analysis of arabic tweets using supervised machine learning," *Proc. - 2020 Int. Conf. Promis. Electron. Technol. ICPET 2020*, pp. 89–93, Dec. 2020, doi: 10.1109/ICPET51420.2020.00025.

[17] W. Al-Sorori *et al.*, "Arabic Sentiment Analysis towards Feelings among Covid-19 Outbreak Using Single and Ensemble Classifiers," pp. 1–6, Nov. 2021, doi: 10.1109/ITSS-IOE53029.2021.9615256.

[18] N. F. Alshammari and A. A. Almansour, "Aspect-based Sentiment Analysis for Arabic Content in Social Media," *2nd Int. Conf. Electr. Commun. Comput. Eng. ICECCE 2020*, Jun. 2020, doi: 10.1109/ICECCE49384.2020.9179327.

[19] H. Elfaik and E. H. Nfaoui, "Deep attentional bidirectional LSTM for arabic sentiment analysis in Twitter," *2021 1st Int. Conf. Emerg. Smart Technol. Appl. eSmarTA 2021*, Aug. 2021, doi: 10.1109/ESMARTA52612.2021.9515751.

[20] A. Alharbi, M. Kalkatawi, and M. Taileb, “Arabic Sentiment Analysis Using Deep Learning and Ensemble Methods,” *Arab. J. Sci. Eng. 2021 469*, vol. 46, no. 9, pp. 8913–8923, May 2021, doi: 10.1007/S13369-021-05475-0.

[21] M. Fawzy, M. W. Fakhr, and M. A. Rizka, “Word Embeddings and Neural Network Architectures for Arabic Sentiment Analysis,” *16th Int. Comput. Eng. Conf. ICENCO 2020*, pp. 92–96, Dec. 2020, doi: 10.1109/ICENCO49778.2020.9357377.

[22] M. Mhamed, R. Sutcliffe, X. Sun, J. Feng, E. Almekhlafi, and E. A. Retta, “A Deep CNN Architecture with Novel Pooling Layer Applied to Two Sudanese Arabic Sentiment Datasets,” Jan. 2022, Accessed: Jun. 03, 2022. [Online]. Available: http://arxiv.org/abs/2201.12664.

Journal of Artificial Intelligence and Data Science (JAIDA)
e-ISSN: 2791-8335
https://dergipark.org.tr/pub/jaida

Vol. 2, No. 1, pp. 31-42, 2022
Research Article

A Novel Approach to Improve Tensile Strength of Al/Mg Hybrid Friction Stir welding Joint by Stochastic Optimization

Onur AYDIN [1], Elif GÜLTÜRK [2,*]

[1] Izmir Katip Celebi University, Department of Mechanical Engineering, Izmir, Turkey
[2] Kocaeli University, Department of Mechanical Engineering, Kocaeli, Turkey

Abstract

Ultrasonic-stationary shoulder-assisted friction stir welding is a novel hybrid welding technique that reveals promising prospects in joining Al/Mg dissimilar alloys. This study aims to develop a design procedure for optimizing the mechanical property of the Al/Mg hybrid friction stir welding joint. For this purpose, firstly, different nonlinear neuro-regression analysis has been performed in order to overcome insufficient approaches for modeling, designing, and optimizing mechanical property in Friction stir welding joint. Then, stochastic optimization methods were performed to model the friction stir welding process. Ultrasonic Power, Welding Speed, and Rotational Velocity are the three most essential criteria that have been used as indicators of process performance. The response characteristic can be predicted as ultimate tensile strength. After calculating the $R^2_{training}$, $R^2_{testing}$, $and\ R^2_{validation}$ values, the limits of the nonlinear models are examined to see whether the model is acceptable for optimization. The best approach model was the second-order trigonometric multiple nonlinear (SOTN) model. In the optimization step, four different Modified Stochastic Optimization Algorithms, including Random Search (MRS), Simulated Annealing (MSA), Nelder Mead (MNM), and differential equations (MDE) methods, were used. It has been observed that the different scenario types and the constraints chosen for the design variables are effective in the optimization results obtained using three different scenarios. Results showed that the maximum tensile strength was 182.301 MPa when ultrasonic power was selected as 186.938 W, 40.6854 mm/min for welding speed, and 1075.34 rpm for rotation speed.
Keywords: Friction stir welding; tensile strength; neuro-regression analysis; stochastic optimization.

1. Introduction

In the current production technology, the demand for high-strength and low-weight structures has increased the need for lightweight hybrid materials. Aluminum (Al) and Magnesium (Mg) alloys, known as commercial metals, play a critical role in the automotive, aerospace, and shipbuilding industries because these materials have high specific strength and formability [1,2]. The widespread use of Al / Mg alloys has increased the importance of the reliable coupling of these alloys. However, due to the formation of intermetallic compounds (IMCs) caused by mental melting and re-solidification during the welding process, it is problematic to combine Al / Mg alloys with standard fusion welding [3-6]. Intermetallic compounds (IMCs) are ordered phases with distinct crystal structures and characteristics than elemental metals. They can be binary, ternary, or polymetallic. Because dissimilar alloys usually have differing atom diameters, crystal structures, and electronegativities, IMCs quickly develop in joints when they are joined. In addition, the ductility and brittleness of IMC are generally poor. When a joint is subjected to external stresses, a fracture can quickly form and spread within the IMC, causing the joint's mechanical qualities to weaken [7]. As a result, when combining different alloys, IMC formation must be avoided. Friction stir welding has been extensively researched as a solid-state welding technology for joining dissimilar materials, such as Ti/Al, Al/St, Al/thermoplastic, and different polymer matrix composites [8-11]. Because of the low peak welding temperature, since it can prevent the development of Al-Mg IMCs, Friction Stir Welding (FSW) is proven to be superior in connecting Al/Mg alloys.

Nonetheless, FSW cannot entirely remove IMCs, limiting the amount of joint tensile strength that may be increased. Therefore, FSW weldability, which is improved by using an additional tool or extra energy, has recently been a growing trend. Stationary Shoulder Friction Stir Welding (SSFSW) is a novel branch of FSW that uses external stationery [12]. By reducing flash and shoulder markings, the outer stationary shoulder optimizes joint formation, increases material flow, and reduces heat input through its heat sink effect. As mechanical energy, the composition and size of Al-Mg IMCs are influenced by ultrasonic vibration. Lv et al. [13] investigated the intermetallic compound layers of friction stir welded Al-Mg joints without and with ultrasonic vibrations. Results showed that during welding Al/Mg dissimilar alloys, ultrasonic may also enhance material flow and reduce material adherence [14]. A novel hybrid welding process of ultrasonic aided SSFSW (U-SSFSW) is created based on the previous two approaches to accomplish the combined benefits of the ultrasonic and stationary shoulder

*Corresponding author e-mail address: elifgulturk@gmail.com

Received: 18/05/2022; Accepted: 27/06/2022

[15]. Thus, in ultrasonic welding of Al/Mg dissimilar alloys, it can improve material flow while reducing material adhesion.

Many experiment methodologies, such as response surface methodology [16] and the Taguchi method [17], have been included in the modeling and parameter optimization of the FSW process in recent years. Because of its self-learning and prediction skills, artificial neural networks (ANN) are frequently used in mathematical modeling for monitoring and assessment applications. ANN is more suited to constructing nonlinear mathematical techniques to simulate and determine outputs by inputs than the response surface approach and Taguchi method [18]. A training step is required to complete self-learning and ANN predicting. Backpropagation (BP) is now the most common training algorithm utilized in ANN, according to published research, based on accuracy and quick response [19]. However, this algorithm's gradient approach for weight correcting may result in a local optimum, where the searching space cannot leap off during the training step [20]. This problem is solved through algorithm optimization. Therefore, several society intelligence algorithms have been developed to ensure the suitability of existing optimization techniques and to provide practical simulation in complex multi-parameter optimizations, such as Particle Swarm optimization [21], Artificial Bee Colony algorithm [22], Imperial Competitive Algorithm [23] and Brainstorm optimization [24]. Verma et al. [25] used an Artificial Neural Network to investigate the influence of FSW parameters which are rotational speed and travel speed, and artificial aging of the characteristics of AA7004 alloy for the first time. The results show that a 320 rpm and 1 mm/s travel speed gives 341 MPa maximum strength and joint efficiency of 80 percent. Also, they have caused re-precipitation of precipitates in the weld zone, which has improved joint efficiency by 59 to 80 percent when as-welded samples are aged under 150 °C for 24 hours. Medhi et al. [26] tried to find the best welding inputs for combining two different materials using the FSW method to produce high-quality joints. They worked on a theory that combines the exploration and exploitation capabilities of the non-dominated sorting genetic algorithm-II (NSGA-II) with the Technique for Order of Preference by Similarity to Ideal Solution (TOPSIS) technique. They observed the increase in ultimate tensile strength, hardness, and impact energy. Liu et al. [27] used ultrasonic-assisted friction stir welding (UaFSW) based on a fixed shoulder system to join 6061-T6 aluminum alloy with AZ31B magnesium alloy to reduce or eliminate the disadvantages caused by continuous IMCs. Their studies determined the maximum tensile strength and elongation of the UaFSW joint were 152.4 MPa and 1.9 percent, respectively. These values were 17 MPa and 0.8 percent higher than the conventional joints. Song et al. [28] worked to combine the dissimilar alloys of AZ31B Mg and 6061-T6 Al, and U-SSFSW was utilized. The correlations between the design parameters of welding and rotating speeds and ultrasonic power and the objectives of ultimate tensile strength of US-SSFSW joints were modeled using a Radial Basis Function Neural Network (RBFNN). The results showed that the RBFNN-GWO system's enhanced design inputs provide the highest ult. tensile strength of 158 MPa.

This study aims to obtain the optimal process parameters that give the maximum ultimate tensile strength in the friction stir welding joints with a novel optimization approach. The design variables were selected as Ultrasonic Power, Welding Speed, and Rotational Velocity; the objective function of the introduced mathematical optimization problems was also ultimate tensile strength. We used the experimental data from the study [30] to carry out this approach. First, ten different regression models were performed, and the validity of the models was evaluated using $R^2_{training}$, $R^2_{testing}$, and $R^2_{validation}$ values. Then optimization process was applied using modified Random Search (MRS), Simulated Annealing (MSA), Nelder Mead (MNM), and Differential Equations (MDE) Algorithms for three different optimization scenarios.

2. Materials and Method

2.1 Modelling

In the current research approach, neuro-regression approach has been applied to obtain the most efficient values for the parameters and the best mathematical model [29]. In this method, all data is divided into three sections, each containing 80%, 15%, and 5% of the total data, respectively—the first section is used for training, the second for testing, and the third for validation. The training process minimizes experimental and predicted value errors, modifying the regression models and their coefficients, as given in Table 1. First, this procedure provides information about the predictive capacity of the candidate models. Second, the adherence of candidate models to predicted values should be checked to determine whether the model is exact. In this section, the maximum and minimum values of models in the given range for each design variable are calculated after obtaining appropriate models from $R^2_{training}$, $R^2_{testing}$, and $R^2_{validation}$. Furthermore, this technique examines if the chosen models satisfy various realistic requirements.

Table 1. *Multiple Regression Model Types[29]*

Model Name	*Nomenclature*	*Formula*
Multiple Linear	L	Y = a[1] + a[2] x1 + a[3] x2 + a[4] x3
Multiple Linear Rational	LR	Y = (a[1] + a[2] x1 + a[3] x2 + a[4] x3)/(b[1] + b[2] x1 + b[3] x2 + b[4] x3)
Second Order Multiple Linear	SON	Y = a[1] + a[2] x1 + a[3] x2 + a[4] x3 + a[5] x1^2 + a[6] x1 x2 + a[7] x2^2 + a[8] x1 x3 + a[9] x2 x3 + a[10] x3^2
Second-Order Multiple Nonlinear Rational	SONR	Y = (a[1] + a[2] x1 + a[3] x2 + a[4] x3 + a[5] x1^2 + a[6] x2^2 + a[7] x3^2 + a[8] x1 x2 + a[9] x1 x3 + a[10] x2 x3)/(b[1] + b[2] x1 + b[3] x2 + b[4] x3 + b[5] x1^2 + b[6] x2^2 + b[7] x3^2 + b[8] x1 x2 + b[9] x1 x3 + b[10] x2 x3)
Third Order Multiple Nonlinear	TON	Y = a[1] + a[2] x1 + a[3] x2 + a[4] x3 + a[5] x1^2 + a[6] x2^2 + a[7] x3^2 + a[8] x1 x2 + a[9] x1 x3 + a[10] x2 x3 + a[11] x1^3 + a[12] x2^3 + a[13] x3^3 + a[14] x1^2 x2 + a[15] x2^2 x3 + a[16] x3^2 x1 + a[17] x3^2 x2 + a[18] x1 x2 x3
First Order Trigonometric Multiple Nonlinear	FOTN	Y = a[1] + a[2] Sin[x1] + a[3] Sin[x2] + a[4] Sin[x3] + a[5] Cos[x1] + a[6] Cos[x2] + a[7] Cos[x3]
First Order Trigonometric Multiple Nonlinear Rational	FOTNR	Y = (a[1] + a[2] Sin[x1] + a[3] Sin[x2] + a[4] Sin[x3] + a[5] Cos[x1] + a[6] Cos[x2] + a[7] Cos[x3])/(b[1] + b[2] Sin[x1] + b[3] Sin[x2] + b[4] Sin[x3] + b[5] Cos[x1] + b[6] Cos[x2] + b[7] Cos[x3])
Second Order Trigonometric Multiple Non-linear	SOTN	Y = a[1] + a[2] Sin[x1] + a[3] Sin[x2] + a[4] Sin[x3] + a[5] Cos[x1] + a[6] Cos[x2] + a[7] Cos[x3] + a[8] Sin[x1]^2 + a[9] Sin[x2]^2 + a[10] Sin[x3]^2 + a[11] Cos[x1]^2 + a[12] Cos[x2]^2 + a[13] Cos[x3]^2
Second Order Trigonometric Multiple Nonlinear Rational	SOTNR	Y = (a[1] + a[2] Sin[x1] + a[3] Sin[x2] + a[4] Sin[x3] + a[5] Cos[x1] + a[6] Cos[x2] + a[7] Cos[x3] + a[8] Sin[x1]^2 + a[9] Sin[x2]^2 + a[10] Sin[x3]^2 + a[11] Cos[x1]^2 + a[12] Cos[x2]^2 + a[13] Cos[x3]^2)/(b[1] + b[2] Sin[x1] + b[3] Sin[x2] + b[4] Sin[x3] + b[5] Cos[x1] + b[6] Cos[x2] + b[7] Cos[x3] + b[8] Sin[x1]^2 + b[9] Sin[x2]^2 + b[10] Sin[x3]^2 + b[11] Cos[x1]^2 + b[12] Cos[x2]^2 + b[13] Cos[x3]^2)
Third Order Multiple Nonlinear Trigonometric	TOTN	Y = a[1] + a[2] Sin[x1] + a[3] Sin[x2] + a[4] Sin[x3] + a[5] Sin[x1]^2 + a[6] Sin[x2]^2 + a[7] Sin[x3]^2 + a[8] Sin[x1 x2] + a[9] Sin[x1 x3] + a[10] Sin[x2 x3] + a[11] Sin[x1]^3 + a[12] Sin[x2]^3 + a[13] Sin[x3]^3 + a[14] Sin[x1^2 x2] + a[15] Sin[x2^2 x3] + a[16] Sin[x3^2 x1] + a[17] Sin[x3^2 x2] + a[18] Sin[x1 x2 x3]

2.2 Optimization

Optimization is obtaining the most appropriate design by minimizing or maximizing the specified single or multi-objective that corresponds to all constraints.

There are two types of optimization techniques: traditional and non-traditional. Only continuous and differentiable functions are suitable for traditional optimization approaches. Traditional optimization techniques cannot be used in their specificity in engineering designs because they work on continuous and differentiable functions. Therefore, stochastic optimization methods such as genetic algorithms (GA), simulated annealing (SA), and particle swarm (PS) are more convenient for engineering applications. However, due to the characteristics of stochastic methods, correct solutions cannot be reached. Using more than one method with different principles for the same optimization problem enhances the dependableness of the solution. In this study, different optimization scenarios, including some problems of optimization problems, were used. Four different stochastic optimization algorithms were used to determine optimal process parameters. These algorithms are the Modified Nelder-Mead (MNM), Modified Differential Evolution (MDE), Modified Simulated Annealing (MSA), and Modified Random Search (MRS) [29].

2.2.1. Nelder-Mead Algorithm

The Nelder-Mead optimization technique is a fundamental direct search approach. As a result, no derivative information is required, and the function's reduction begins with simplex. The iteration continues until the simplex is reached, which becomes flat. It signifies that the function's outcome is almost identical at all vertices. The Nelder-Mead algorithm's iteration phases include ordering, centroid, and transformation [29].

2.2.2. Differential Evolution Algorithm

The differential evolution optimization method is one of the appropriate stochastic optimizations. It may determine the best solution in complex structured composite design challenges. Instead of iterating over solutions, it deals with a population of them. As a result, even if the differential evolution technique does not attain globally optimal points with all optimization problems, it is considered resilient and efficient [29].

2.2.3. Simulated Annealing

The simulated annealing optimization technique is another common search technique based on the actual annealing of metals. During the melting process, the material transfers to a lower energy level and becomes stiff. The algorithm is superior at finding the global optimum because of its inherent structure. In addition, it can handle optimization problems that are continuous, mixed-integer, or discrete [29].

2.2.4. Random Search Algorithm

The random search optimization technique is a standard random reach algorithm to generate a population of unpredictably placed starting spots. It utilizes a local optimization strategy to reach a local extremum point from each starting position. As a solution, the best local minimum is chosen. Specific booster subroutines, like the conjugate gradient, main axis, Levenberg-Marquardt, Newton, Quasi-Newton, and nonlinear interior-point approach, are utilized in the recommended version of the algorithm to optimize the values of all parameters for the objective function. In this stage, the fitness function is evaluated with symbolic variables, and then the method is repeated [29].

2.3 Problem Definition

The optimal design of ultrasonic power (W), welding speed (mm/min), and rotational speed (rpm) giving the maximum tensile strength value in a friction stir welding joint, is realized as follows. Experimental data from the reference work [30] to be used in modeling are shown in Table 2. The optimization procedure is conducted by Mathematica [49] program.

- Ten different mathematical models are implemented to provide friction stir source data and the limitations and suitability of the functions are checked for the values of $R^2_{training}$, $R^2_{testing}$, and $R^2_{validation}$.
- Optimization was performed using four different modified stochastic optimization algorithms, namely, Differential Evolution (DE), Simulated Annealing (SA), Random Search (RS), and Nelder-Mead (NM), for three different optimization scenarios using appropriate models.

2.4 Optimization Scenarios

Three different design-optimization scenarios have been introduced to define the process. The following logic was used while creating the optimization scenarios:

Scenario 1

In this scenario, the objective function defines the ultimate tensile strength, the ranges of the design variables are chosen considering the experimental data, and it was possible for each variable to take any real number. For example, 0 < ultrasonic power (W) < 1800, 30 < welding speed (mm/min) <80 and 900 < rotational speed (rpm) < 1200. The aim is to maximize the tensile strength of the weld material. In addition, the limits of the objective function can be calculated with this approach.

Scenario 2

Relying on the proposed experimental setup, the more specific optimization problem can also be identified as involving the optimization of objective functions, all design constraints are assumed to be real numbers at the

intervals: 0 < ultrasonic power (W) < 1800, 30 < welding speed (mm/min) < 80, and 900 < rotational velocity (rpm) < 1200. Design variables are forced to be integers, provided they comply with engineering requirements.

Scenario 3

The more detailed optimization issue may alternatively be stated as maximum tensile strength; design variables some values are chosen from experimental data and constraints are ultrasonic power ∈ {0, 600, 1000, 1400, 1800}; welding speed ∈ {30, 40, 50, 60, 70, 80}; rotational speed ∈ {900, 1000, 1100, 1200}. This scenario will allow seeing the optimum results that the proposed model produces only under certain conditions.

Table 2. *Friction Stir Welding Process Parameters[30]*

Run	***Ultrasonic Power (W)***	***Welding Speed (mm/min)***	***Rotational velocity (rpm)***	***Ultimate Tensile Strength (MPa)***
1	0	30	900	71
2	0	30	1000	77
3	0	30	1100	53
4	0	40	900	109
5	0	40	100	126
6	0	40	1200	66
7	0	50	900	122
8	0	50	100	134
9	0	50	1100	119
10	0	60	900	147
11	0	60	1000	137
12	0	60	1100	117
13	0	70	1000	118
14	0	70	1100	110
15	0	80	1100	79
16	600	30	1000	94
17	600	60	1000	131
18	600	80	1000	58
19	1000	30	1000	115
20	1000	60	1000	133
21	1000	80	1000	87
22	1400	30	1000	13
23	1400	60	1000	152
24	1400	80	1000	134
25	1800	30	1000	92
26	1800	60	1000	120
27	1800	80	1000	80

3. Results and Discussion

In this study, ten different regression models for ultrasonic power, welding speed, and rotational speed in friction stir welding joints were tested with three different 'goodness of the fit' measures, , $R^2_{training}$, $R^2_{testing}$, $R^2_{validation}$. Table 3 shows the mathematical models used in the neuro-regression analysis for the related process parameters in friction stir welding connections. Optimum parameters x1, x2, and x3 correspond to ultrasonic power, welding speed, and rotational speed. Models with the highest R^2 values define the relationship between response and reality better than other models. When the table is examined, it is seen that $R^2_{testing}$, and $R^2_{validation}$ values in some models are not close to 1 or have negative values. This situation also showed that high

$R^2_{training}$ values alone could not describe the phenomenon. In addition, negative coefficients indicate that the model cannot be described as statistically significant. Accordingly, the results show that the most reliable model is Quadratic Trigonometric Multiple Nonlinear (SOTN), as the values of $R^2_{training}$, $R^2_{testing}$, and $R^2_{validation}$ are 0.995, 0.806, and 0.846, respectively. When the SOTN model is examined in terms of tensile strength, the negative minimum tensile strength value may not be considered appropriate. However, considering the models where the minimum or maximum ultimate tensile strength values are asymptotically infinite, this can be considered positive for the stability of the model. As a result, tensile strength values are acceptable and within reasonable limits.

Optimization results of the process parameters in ultimate tensile strength according to three different scenarios with different constraints are presented in Table 4. Using the SOTN model, design parameters that maximize tensile strength were determined for each scenario using four different algorithms: MRS, MDE, MSA, and MNM. The intervals of scenario 1 were chosen considering the limits of the experimental study, and each variable took a real value. It obtained more successful results in terms of tensile strength in this scenario.

While the maximum tensile strength was the same in MRS, MNM, and MDE algorithms, MSA was different. In addition, it is seen that the design parameters that provide the maximum tensile strength are given within limits and as real numbers. In Scenario 2, some design variables were forced to be integers while getting the optimization results, provided they comply with the engineering requirements. The results showed that the MDE algorithm for scenario 2 gives better results than the other three algorithms. In scenario 3, the optimum results produced by the model were values that will be seen only under certain conditions, and the final tensile strength values for all algorithms are the same. The optimization results of the ultimate tensile strength parameter show that the maximum tensile strength in the three algorithms of scenario 1 (MRS, MNM, MDE) is 182.301 MPa, and in the MDE algorithm of the second scenario, 182.237MPa. However, it can be said that the insufficient solutions in the 2nd and 3rd scenarios are due to the restrictions made compared to the Scenario 1. In general, it can be said that all algorithms have acceptable results within limitations, although it is clear that MDE produces more successful outcomes in scenarios 1 and 2. Finally, the results reveal that the Ultimate Tensile Strength can be maximized to 182.301MPa for the following optimal conditions; Ultrasonic Power: 186.938 W, Welding Speed: 40.6854 mm/m inch, Rotation Speed: 1075.3.

Table 3. *Results of the Neuro-regression models in terms of fitting performance and boundedness.*

Models	$R^2_{training}$	$R^2_{testing}$	$R^2_{validation}$	Max. Ultimate Tensile Strength	Min. Ultimate Tensile Strength
Y = 231.84 + 0.000495499 x1 + 0.328724 x2 - 0.133415 x3	0.977	-0.246	0.352	138.956	65.587
Y = (2.1144*10^-8 + 3227.18 x1 + 2.46248*10^-9 x2 - 9.74408*10^-11 x3)/(1.90369*10^-11 + 27.7249 x1 + 2.06805*10^-11 x2 - 6.7093*10^-13 x3)	0.990	-1.753	-0.552	116.4	116.4
Y = -1140.89 - 0.0163631 x1 + 0.0000410955 x1^2 + 6.47544 x2 + 3.00384*10^-6 x1 x2 - 0.0729875 x2^2 + 2.20297 x3 - 0.0000163631 x1 x3 + 0.00154806 x2 x3 -0.00114843 x3^2	0.995	-1.2903	0.884	209.015	40.685
Y = (2.01217 + 12.7823 x1 - 8352.59 x1^2 + 30.4753 x2 - 50552.6 x1 x2 + 769.567 x2^2 + 760.715 x3 + 11783.3 x1 x3 + 20432.3 x2 x3 - 198.539 x3^2)/(46.4385 + 1.09301 x1 - 69.1329 x1^2 + 2368.52 x2 - 371.918 x1 x2 + 4523.71 x2^2 - 3777.59 x3 + 94.0089 x1 x3 - 319.732 x2 x3 + 14.8251 x3^2)	0.995	0.004	0.975	2.289*10^12	-6.644*10^15
Y = -451.465 + 0.042831 x1 - 0.0000123597 x1^2 - 4.05251*10^-8 x1^3 - 53.6399 x2 - 0.00196325 x1 x2 + 2.66068*10^-6 x1^2 x2 - 0.577702 x2^2 + 0.00234579 x2^3 + 2.77865 x3 + 0.000042831 x1 x3 + 0.163982 x2 x3 - 1.96325*10^-6 x1 x2 x3 + 0.0001186 x2^2 x3 - 0.0051376 x3^2 + 4.2831*10^-8 x1 x3^2 - 0.0000818925 x2 x3^2 + 2.38379*10^-6 x3^3	0.999	-1.302	0.983	199.449	-14.859

Y = 46.9925 - 10.1483 Cos[x1] - 4.58153 Cos[x2] + 37.2763 Cos[x3] - 8.31784 Sin[x1] + 11.8687 Sin[x2] + 77.3452 Sin[x3]	0.982	-0.415	0.436	158.696	-64.711
Y = (-5372.22 + 102.542 Cos[x1] - 189.613 Cos[x2] + 5924.52 Cos[x3] + 1.28016 Sin[x1] - 604.597 Sin[x2] + 1654.09 Sin[x3])/(-42.3369 + 0.884183 Cos[x1] - 1.73952 Cos[x2] + 47.6956 Cos[x3] + 0.017317 Sin[x1] - 4.97124 Sin[x2] + 12.0455 Sin[x3])	0.999	-0.137	-0.400	1.962*10^13	-4.396*10^11
Y = 5.11515 + 1.02361 Cos[x1] - 1.76996 Cos[x1]^2 - 1.41558 Cos[x2] + 27.9902 Cos[x2]^2 + 11.9876 Cos[x3] + 43.7613 Cos[x3]^2 - 12.4817 Sin[x1] + 31.5856 Sin[x1]^2 + 12.1898 Sin[x2] - 10.7053 Sin[x2]^2 + 114.622 Sin[x3] - 18.5691 Sin[x3]^2	0.995	0.806	0.846	182.301	-155.226

Y = (20.8944 + 7.67565 Cos[x1] + 0.826635 Cos[x1]^2 + 77.4142 Cos[x2] + 41.7063 Cos[x2]^2 + 23.7181 Cos[x3] + 25.2186 Cos[x3]^2 + 12.9568 Sin[x1] + 21.0678 Sin[x1]^2 + 35.4982 Sin[x2] -19.8119 Sin[x2]^2 + 2.71789 Sin[x3] - 3.32416 Sin[x3]^2)/(-0.204871 + 0.118014 Cos[x1] + 0.312046 Cos[x1]^2 + 0.637254 Cos[x2] + 0.632187 Cos[x2]^2 + 0.416064 Cos[x3] + 0.0173435 Cos[x3]^2 + 0.112826 Sin[x1] + 0.483083 Sin[x1]^2 + 0.274419 Sin[x2] + 0.162942 Sin[x2]^2 - 1.06296 Sin[x3] + 0.777785 Sin[x3]^2)	0.999	-19.814	0.273	2.002*10^13	-2.322*10^15
Y = 116.852 - 8.06062 Sin[x1] + 13.2376 Sin[x1]^2 - 12.1903 Sin[x1]^3 + 101.768 Sin[x2] - 127.618 Sin[x2]^2 - 129.696 Sin[x2]^3 - 6.4981 Sin[x1 x2] + 24.6749 Sin[x1^2 x2] + 60.2451 Sin[x3] + 204.718 Sin[x3]^2 - 232.073 Sin[x3]^3 - 25.3439 Sin[x1 x3] - 21.149 Sin[x2 x3] - 3.96789 Sin[x1 x2 x3] - 16.2345 Sin[x2^2 x3] + 15.4914 Sin[x1 x3^2] - 10.6171 Sin[x2 x3^2]	1.	-0,405	0.868	577.338	-67.726

Table 4. *Results of optimization problems for the selected models.*

Objective Functions	*Scenario Number*	*Constraints*	*Optimization Algorithm*	*Ultimate Tensile Strength*	*Suggested Design*
SOTN	1	0 < x1 < 1800, 30 < x2 < 80, 900 < x3 < 1200	MSA	173.611	x1 = 1299.06, x2 = 75.559, x3 = 900.
			MRS	182.301	x1 = 186.938, x2 = 40.685, x3 = 1075.34
			MNM	182.301	x1 = 557.646, x2 = 65.818, x3 = 1100.47
			MDE	182.301	x1 = 903.221, x2 = 59.535, x3 = 1031.36
	2	0 < x1 < 1800, 30 < x2 < 80, 900 < x3 < 1200, {x1, x2, x3} \[Element] Integers	MSA	177.183	x1 = 300, x2 = 47, x3 = 1075
			MRS	143.972	x1 = 590, x2 = 66, x3 = 1100
			MNM	169.919	x1 = 614, x2 = 72, x3 = 1100
			MDE	182.237	x1 = 1054, x2 = 47, x3 = 912
	3	x1 == 0 || x1 == 600 || x1 == 1000 || x1 == 1400 || x1 == 1800, x2 == 30 || x2 == 40 || x2 == 50 || x2 == 60 || x2 == 70 || x2 == 80, x3 == 900 || x3 == 1000 || x3 == 1100 || x3 == 1200	MSA	167.648	1 = 1400., x2 = 50., x3 = 1000.
			MRS	167.648	x1 = 1400, x2 = 60, x3 = 1000
			MNM	167.648	x1 = 1400, x2 = 60, x3 = 1000
			MDE	167.648	x1 = 1400, x2 = 60, x3 = 1000

4. Conclusions

This paper aimed to design optimization based on nonlinear multiple neuro regression analysis to maximize ultimate tensile strength in friction stir welding joints using Mathematica software.

After modeling the ultimate tensile strength using process variables, the following conclusions may be drawn:

- This is the first study on the optimal design of the operating parameters of the friction stir welding joint with a comprehensive neuro-regression analysis.
- 10 different regression models were evaluated, and the most suitable one (SOTN) for the output was selected. The $R^2_{training}$, $R^2_{testing}$, and $R^2_{validation}$ values of the models have acceptable levels.
- It has been shown that neuro-regression models with only high $R^2_{training}$, values are unsuitable and reliable in engineering, even if they give reasonable results. For this reason, it is suggested that $R^2_{testing}$, and $R^2_{validation}$should be close to 1 for real-life applications.
- The optimization results were influenced by the different scenario types and the selection of constraints for design variables.
- Although it is clear that MDE produces more successful results in scenarios 1 and 2, it can be said that all algorithms have acceptable results. Ultrasonic power: 186.938 W, Welding Speed: 40.685 mm/min, and Rotational Velocity: 1075.3 were found for ultimate tensile strength of 182. 301Mpa.
- It has also been shown that trigonometric models (SOTN) can be used to determine the input parameters of friction stir welding joints. Maximizing the ultimate tensile strength with the collaboration of stochastic optimization methods (MDE, MNM, MRS, MSA) is appropriate.

Declaration of Interest

The authors declare that there is no conflict of interest.

References

[1] Ma, Zhongwei, et al. "A general strategy for the reliable joining of Al/Ti dissimilar alloys via ultrasonic assisted friction stir welding." Journal of Materials Science & Technology 35.1 (2019): 94-99.

[2] He, Bin, et al. "Microstructure and mechanical properties of RAFM-316L dissimilar joints by friction stir welding with different butt joining modes." Acta Metallurgica Sinica (English Letters) 33.1 (2020): 135-146.

[3] Chen, Yanbin, Shuhai Chen, and Liqun Li. "Effects of heat input on microstructure and mechanical property of Al/Ti joints by rectangular spot laser welding-brazing method." The International Journal of Advanced Manufacturing Technology 44.3 (2009): 265-272.

[4] Zhong, Y. B., CS and Wu, and G. K. Padhy. "Effect of ultrasonic vibration on welding load, temperature and material flow in friction stir welding." Journal of Materials Processing Technology 239 (2017): 273-283.

[5] Padhy, G. K., C. S. Wu, and S. Gao. "Precursor ultrasonic effect on grain structure development of AA6061-T6 friction stir weld." Materials & Design 116 (2017): 207-218.

[6] Liu, X. C., and C. S. Wu. "Elimination of tunnel defect in ultrasonic vibration enhanced friction stir welding." Materials & Design 90 (2016): 350-358.

[7] Xu, Zhiwu, et al. "Control Al/Mg intermetallic compound formation during ultrasonic-assisted soldering Mg to Al." Ultrasonics Sonochemistry 46 (2018): 79-88.

[8] Xu, W. F., et al. "Abnormal fracture of 7085 high strength aluminum alloy thick plate joint via friction stir welding." Journal of Materials Research and Technology 8.6 (2019): 6029-6040.

[9] Huang, Yongxian, et al. "Self-riveting friction stir lap welding of aluminum alloy to steel." Materials Letters 185 (2016): 181-184.

[10] Huang, Yongxian, et al. "Joining of carbon fiber reinforced thermoplastic and metal via friction stir welding with co-controlling shape and performance." Composites Part A: Applied Science and Manufacturing 112 (2018): 328-336.

[11] Huang, Yongxian, et al. "Friction stir welding/processing of polymers and polymer matrix composites." Composites Part A: Applied Science and Manufacturing 105 (2018): 235-257.

[12] Ji, S. D., et al. "Formation and mechanical properties of stationary shoulder friction stir welded 6005A-T6 aluminum alloy." Materials & Design (1980-2015) 62 (2014): 113-117.

[13] Lv, X. Q., C. S. Wu, and G. K. Padhy. "Diminishing intermetallic compound layer in ultrasonic vibration enhanced friction stir welding of aluminum alloy to magnesium alloy." Materials Letters 203 (2017): 81-84.

[14] Liu, Zhenlei, Shude Ji, and Xiangchen Meng. "Improving joint formation and tensile properties of dissimilar friction stir welding of aluminum and magnesium alloys by solving the pin adhesion problem." Journal of Materials Engineering and Performance 27.3 (2018): 1404-1413.

[15] Liu, Zhenlei, et al. "Improving tensile properties of Al/Mg joint by smashing intermetallic compounds via ultrasonic-assisted stationary shoulder friction stir welding." Journal of Manufacturing Processes 31 (2018): 552-559.

[16] Kim, Weon-Kyong, Si-Tae Won, and Byeong-Choon Goo. "A study on mechanical characteristics of the friction stir welded A6005-T5 extrusion." International Journal of Precision Engineering and Manufacturing 11.6 (2010): 931-936.

[17] Koilraj, M., et al. "Friction stir welding of dissimilar aluminum alloys AA2219 to AA5083–Optimization of process parameters using Taguchi technique." Materials & Design 42 (2012): 1-7.
[18] Benyounis, K. Y., and Abdul-Ghani Olabi. "Optimization of different welding processes using statistical and numerical approaches–A reference guide." Advances in engineering software 39.6 (2008): 483-496.
[19] Darzi Naghibi, Hamed, Mohsen Shakeri, and Morteza Hosseinzadeh. "Neural network and genetic algorithm based modeling and optimization of tensile properties in FSW of AA 5052 to AISI 304 dissimilar joints." Transactions of the Indian Institute of Metals 69.4 (2016): 891-900.
[20] Zhou, Nan, et al. "Genetic Algorithm Coupled with the Neural Network for Fatigue Properties of Welding Joints Predicting." J. Comput. 7.8 (2012): 1887-1894.
[21] Kennedy, James, and Russell Eberhart. "Particle swarm optimization." Proceedings of ICNN'95-international conference on neural networks. Vol. 4. IEEE, 1995..
[22] Karaboga, Dervis, and Bahriye Basturk. "A powerful and efficient algorithm for numerical function optimization: artificial bee colony (ABC) algorithm." Journal of global optimization 39.3 (2007): 459-471.
[23] Atashpaz-Gargari, Esmaeil, and Caro Lucas. "Imperialist competitive algorithm: an algorithm for optimization inspired by imperialistic competition." 2007 IEEE congress on evolutionary computation. Ieee, 2007.
[24] Shi, Yuhui. "An optimization algorithm based on brainstorming process." Emerging Research on Swarm Intelligence and Algorithm Optimization. IGI Global, 2015. 1-35.
[25] Verma, A., B. Kotteswaran, and T. Shanmugasundaram. "Effect of Welding Parameters and Artificial Aging on Mechanical Properties of Friction Stir Welded AA 7004 Alloys: Experimental and Artificial Neural Network Simulation." Metallography, Microstructure, and Analysis 10.4 (2021): 515-524.
[26] Medhi, Tanmoy, et al. "An intelligent multi-objective framework for optimizing friction-stir welding process parameters." Applied Soft Computing 104 (2021): 107190.
[27] Liu, Zhenlei, et al. "Improving tensile properties of Al/Mg joint by smashing intermetallic compounds via ultrasonic-assisted stationary shoulder friction stir welding." Journal of Manufacturing Processes 31 (2018): 552-559.
[28] Song, Qi, et al. "Improving joint quality of hybrid friction stir welded Al/Mg dissimilar alloys by RBFNN-GWO system." Journal of Manufacturing Processes 59 (2020): 750-759.
[29] Aydin, L., Artem, H.S., Oterkus, S. (Editors). Designing Engineering Structures Using Stochastic Optimization Methods. CRC Press Taylor & Francis Group. 2020
[30] Hu, Wei, et al. "Improving the mechanical property of dissimilar Al/Mg hybrid friction stir welding joint by PIO-ANN." Journal of Materials Science & Technology 53 (2020): 41-52.

Journal of Artificial Intelligence and Data Science (JAIDA)
e-ISSN: 2791-8335
https://dergipark.org.tr/pub/jaida

Vol. 2, No. 1, pp. 43-52, 2022
Research Article

Optimization of Wire Electrical Discharge Machining (WEDM) Process Parameters Using Neuro-Regression Analysis for Fabrication of Precision Electrodes with Complex Shapes

Meliha BAŞTÜRK

Volt Elektrik Motor San. ve Tic. A.Ş., Electrical-Electronics Engineer, Kemalpasa, Izmir, Turkey

Abstract
The wire electrical discharge machining (WEDM) process is extremely important in the fabrication of complex electrodes with delicate structures. Identifying optimal operating combinations is a challenge in industry due to the large number of process variables. To overcome this difficulty, neuro-regression analysis was used and optimization was carried out. In this study, the six-parameter WEDM process was first modeled in twelve different regression models using a neuro-regression analysis. These parameters are discharge current, pulse duration, pulse frequency, wire speed, wire tension and dielectric flow rate. In addition, multiple regression model types including linear, quadratic, trigonometric and rational forms were tested in twelve different regression models. Then, optimization study was carried out with four different algorithms to obtain minimum kerf and surface roughness. These algorithms are Nelder-Mead Algorithm, Differential Evolution Algorithm, Simulated Annealing Algorithm and Random Search Algorithm. The study shows that WEDM process parameters can be adjusted to achieve better surface finish and cutting width at the same time. The process is optimized by minimizing kerf and surface roughness. Optimization results are 0.17044 mm for kerf and 3.60393 μm for surface roughness. It is seen that the processing model is suitable and the optimization technique meets the practical requirements.
Keywords: Kerf; neuro-regression analysis; optimization; surface roughness; WEDM.

1. Introduction

WEDM technology is based on the principle of electro-erosion. During this process, metals corrode each other. With the control of the electro-erosion process, it may be possible to manufacture conductive materials of complex shapes. It is a very popular and widely used technology for cutting and manufacturing plastic molds, which is also used in the production of gear wheels and machine parts. WEDM is preferred by researchers/industry to save time, energy and money with the spread of mechanization and the development of technology [1].

Many investigations have been performed in the field of WEDM, which include process modeling studies. Mouralova et al. [2] investigated it is important that the kerf width is as small as possible to ensure precision machining. For this reason, the slit was investigated in metallographic sections using light and electron microscopy. Surface roughness is important for the finishing cut of WEDM. Han et al. [3] experimentally investigated the effects of WEDM parameters including pulse time, discharge current, continuous pulse time, pulse interval time, polarity effect, material and dielectric or surface roughness in finishing. Saha and Mondal [4] examined the influence of WEDM parameters such as discharge pulse time, discharge stop time, servo voltage. In addition to experimental studies, combination of Taguchi's robust design concept and principal component analysis were applied to optimize those process parameters. Kumar et al. [5] analyzed the analytical hierarchy process and genetic algorithm studies to determine the best WEDM conditions for hybrid composites. In that research, three response parameters such as metal removal rate, surface roughness and spark gap were considered for process optimization. Shihab [6] used the Box-Behnken design to maximize metal removal rate while achieving low kerf and surface roughness in optimization. He realized the optimum process parameters. A new approach to determinate cutting parameters in WEDM, integrated artificial neural network (ANN), and wolf pack algorithm based on the strategy of the leader (LWPA) proposed by Ming et al. [7]. He presented an ANN-LWPA integration system with multiple fitness functions to solve the modeling problems. Two smart prediction tools, namely general regression neural network (GRNN) and multiple regression analysis (MRA) models, were developed in the research of Majumder and Maity [8]. In that study they predicted and compared some key machinability properties such as average notch width, average surface roughness, and material removal rate. Analysis of variance was performed by Phate et al. [9] to understand the effect of WEDM process parameters on overall WEDM efficiency. WEDM response properties such as surface roughness (Ra), material removal rate and kerf width were considered in that study. The ANN was employed for enhancing the performance of the process. Manjaiah et al. [10] used multi-objective optimization by using Taguchi-based utility approach to optimize Ra.

Corresponding author e-mail address: meliha.basturk98@gmail.com

Received: 12/05/2022; Accepted: 27/06/2022

In this study it is aimed to optimize kerf (cutting width) and surface roughness. Taguchi design and neuro-regression method were used during optimization process. Neuro-regression analysis were performed methodically, including linear, quadratic, trigonometric, logarithmic, and their rational forms. $R^2_{training}$, $R^2_{testing}$ and $R^2_{validation}$ values were checked for the validity of the models. Stochastic optimization methods were used to maximize or minimize the objective functions to optimum values. Finally, different direct search methods (modified differential evaluation, Nelder-Mead [11], random search and simulated annealing algorithms) are methodically performed.

2. Materials and Methods

2.1 Modeling

In the modeling phase, a method combining the use of neuro-regression analysis and ANN was used. In order to apply this method, two different data separation was used. In the first one, all data were divided into three parts. 80% of the data was used for training, 15% for testing, and 5% for validation. In the second one, the same data set were split into two parts as 80% for training and 20% for testing. Moreover 5% validation data was selected from the second part of the data whose percentage was determined as 20% before. Both splitting methods mentioned above were applied and the most suitable method for modeling was chosen. The second is more likely to pass stages. If we explain these stages briefly, the training stage aims to minimize the error between the experimental and predicted values by changing the given regression models and coefficients. The test stage is performed to obtain the prediction results by minimizing the effects of regression model mismatches. It is crucial to check the boundary values with the predicted ones to show whether the model is realistic or not. After obtaining suitable models for training and testing, the maximum and minimum values of the given models were calculated for each design variable. Equations of twelve different regression models are given in Table 1. Multiple regression models and types were used including linear, quadratic, trigonometric, logarithmic and rational forms [12].

Table 1. *Regression models name with nomenclature – formula.*

Model Name	Nomenclature	Formula
Multiple Linear	L	a[1] + a[2] x1 + a[3] x2 + a[4] x3 + a[5] x4 + a[6] x5 + a[7] x6
Multiple Linear Rational	LR	(a[1] + a[2] x1 + a[3] x2 + a[4] x3 + a[5] x4 + a[6] x5 + a[7] x6)/(b[1] + b[2] x1 + b[3] x2 + b[4] x3 + b[5] x4 + b[6] x5 + b[7] x6)
Second-Order Multiple Nonlinear	SON	a[1] + a[2] x1 + a[3] x2 + a[4] x3 + a[5] x4 + a[6] x5 + a[7] x6 + a[8] x1^2 + a[9] x2^2 + a[10] x3^2 + a[11] x4^2 + a[12] x5^2 + a[13] x6^2+ 2 a[14] x1 x2 + 2 a[15] x1 x3 + 2 a[16] x1 x4 + 2 a[17] x1 x5 + 2 a[18] x1 x6 + 2 a[19] x2 x3 + 2 a[20] x2 x4 + 2 a[21] x2 x5
Second-Order Multiple Nonlinear Rational	SONR	(a[1] + a[2] x1 + a[3] x2 + a[4] x3 + a[5] x4 + a[6] x5 + a[7] x6 + a[8] x1^2 + a[9] x2^2 + a[10] x3^2 + a[11] x4^2 + a[12] x5^2 + a[13] x6^2 + 2 a[14] x1 x2 + 2 a[15] x1 x3 + 2 a[16] x1 x4 + 2 a[17] x1 x5 + 2a[18] x1 x6 + 2 a[19] x2 x3 + 2 a[20] x2 x4 + 2 a[21] x2 x5)/(b[1] + b[2] x1 + b[3] x2 + b[4] x3 + b[5] x4 + b[6] x5 + b[7] x6 + b[8] x1^2 + b[9] x2^2 + b[10] x3^2 + b[11] x4^2 + b[12] x5^2 + b[13] x6^2 + 2 b[14] x1 x2 + 2 b[15] x1 x3 + 2 b[16] x1 x4 + 2 b[17] x1 x5 + 2 b[18] x1 x6 + 2 b[19] x2 x3 + 2 b[20] x2 x4 + 2 b[21] x2 x5)
First-Order Trigonometric Multiple Nonlinear	FOTN	a[1] + a[2] Sin[x1] + a[3] Sin[x2] + a[4] Sin[x3] + a[5] Sin[x4] + a[6] Sin[x5] + a[7] Sin[x6] + a[8] Cos[x1] + a[9] Cos[x2] + a[10] Cos[x3] + a[11] Cos[x4] + a[12] Cos[x5] + a[13] Cos[x6]
First-Order Trigonometric Multiple Nonlinear Rational	FOTNR	a[1] + a[2] Sin[x1] + a[3] Sin[x2] + a[4] Sin[x3] + a[5] Sin[x4] + a[6] Sin[x5] + a[7] Sin[x6] + a[8] Cos[x1] + a[9] Cos[x2] + a[10] Cos[x3] + a[11] Cos[x4] + a[12] Cos[x5] + a[13] Cos[x6])/(b[1] + b[2] Sin[x1] + b[3] Sin[x2] + b[4] Sin[x3] + b[5] Sin[x4] + b[6] Sin[x5] + b[7] Sin[x6] + b[8] Cos[x1] + b[9] Cos[x2] + b[10] Cos[x3] + b[11] Cos[x4] + b[12] Cos[x5] + b[13] Cos[x6])
Second-Order Trigonometric Multiple Nonlinear	SOTN	a[1] + a[2] Sin[x1] + a[3] Sin[x3]^2 + a[4] Sin[x3]^2 + a[5] Sin[x4]^2 + a[6] Sin[x5]^2 + a[7] Sin[x6]^2 + a[8] Cos[x1] + a[9] Cos[x2] + a[10] Cos[x3] + a[11] Cos[x4] + a[12] Cos[x5] + a[13] Cos[x6] + a[14] Sin[x1] + a[15] Sin[x2] + a[16] Sin[x3] + a[17] Sin[x4] + a[18] Sin[x5] + a[19] Sin[x6] + a[20] Cos[x1]^2 + a[21] Cos[x2]^2 + a[22] Cos[x3]^2 + a[23] Cos[x4]^2 + a[24] Cos[x5]^2 + a[25] Cos[x6]^2
Second-Order Trigonometric Multiple Nonlinear Rational	SOTNR	a[1] + a[2] Sin[x1] + a[3] Sin[x3]^2 + a[4] Sin[x3]^2 + a[5] Sin[x4]^2 + a[6] Sin[x5]^2 + a[7] Sin[x6]^2 + a[8] Cos[x1] + a[9] Cos[x2] + a[10] Cos[x3] + a[11] Cos[x4] + a[12] Cos[x5] + a[13] Cos[x6] + a[14] Sin[x1] + a[15] Sin[x2] + a[16] Sin[x3] + a[17] Sin[x4] + a[18] Sin[x5] + a[19] Sin[x6] + a[20] Cos[x1]^2 + a[21] Cos[x2]^2 + a[22] Cos[x3]^2 + a[23] Cos[x4]^2 + a[24] Cos[x5]^2 + a[25] Cos[x6]^2)/(b[1] + b[2] Sin[x1] + b[3] Sin[x3]^2 + b[4] Sin[x3]^2 + b[5]

		Sin[x4]^2 + b[6] Sin[x5]^2 + b[7] Sin[x6]^2 + b[8] Cos[x1] + b[9] Cos[x2] + b[10] Cos[x3] + b[11] Cos[x4] + b[12] Cos[x5] + b[13] Cos[x6] + b[14] Sin[x1] + b[15] Sin[x2] + b[16] Sin[x3] + b[17] Sin[x4] + b[18] Sin[x5] + b[19] Sin[x6] + b[20] Cos[x1]^2 + b[21] Cos[x2]^2 +b[22] Cos[x3]^2 + b[23] Cos[x4]^2 + b[24] Cos[x5]^2 + b[25] Cos[x6]^2)
First-Order Logarithmic Multiple Nonlinear	FOLN	a[1] + a[2] Log[x1] + a[3] Log[x2] + a[4] Log[x3] + a[5]Log[x4] + a[6] Log[x5] + a[7] Log[x6]
First-Order Logarithmic Multiple Nonlinear Rational	FOLNR	(a[1] + a[2] Log[x1] + a[3] Log[x2] + a[4] Log[x3] + a[5] Log[x4] + a[6] Log[x5] + a[7] Log[x6])/(b[1] + b[2] Log[x1] + b[3] Log[x2] + b[4] Log[x3] + b[5] Log[x4] + b[6] Log[x5] + b[7] Log[x6])
Second-Order Logarithmic Multiple Nonlinear	SOLN	a[1] + a[2] Log[x1] + a[3] Log[x2] + a[4] Log[x3] + a[5] Log[x4] + a[6] Log[x5] + a[7] Log[x6] + a[8] Log[x1 x2] + a[9] Log[x1 x3] + a[10] Log[x1 x4] + a[11] Log[x1 x5] + a[12] Log[x1 x6] + a[13] Log[x2 x3] + a[14] Log[x2 x4] + a[15] Log[x2 x5] + a[16] Log[x2 x6] + a[17] Log[x3 x4] + a[18] Log[x3 x5] + a[19] Log[x3 x5] + a[20] Log[x3 x6] + a[21] Log[x4 x5] + a[22] Log[x4 x6] + a[23] Log[x5 x6] + a[24] Log[x1]^2 + a[25] Log[x2]^2 + a[26] Log[x3]^2 + a[27] Log[x4]^2 + a[28] Log[x5]^2 + a[29] Log[x6]^2
Second-Order Logarithmic Multiple Nonlinear	SOLNR	a[1] + a[2] Log[x1] + a[3] Log[x2] + a[4] Log[x3] + a[5] Log[x4] + a[6] Log[x5] + a[7] Log[x6] + a[8] Log[x1 x2] + a[9] Log[x1 x3] + a[10] Log[x1 x4] + a[11] Log[x1 x5] + a[12] Log[x1 x6] + a[13] Log[x2 x3] + a[14] Log[x2 x4] + a[15] Log[x2 x5] + a[16] Log[x2 x6] + a[17] Log[x3 x4] + a[18] Log[x3 x5] + a[19] Log[x3 x5] + a[20] Log[x3 x6] + a[21] Log[x4 x5] + a[22] Log[x4 x6] + a[23] Log[x5 x6] + a[24] Log[x1]^2 + a[25] Log[x2]^2 + a[26] Log[x3]^2 + a[27] Log[x4]^2 + a[28]Log[x5]^2 + a[29] Log[x6]^2)/(b[1] + b[2] Log[x1] + b[3] Log[x2] + b[4] Log[x3] + b[5] Log[x4] + b[6] Log[x5] + b[7] Log[x6] + b[8] Log[x1 x2] + b[9] Log[x1 x3] + b[10] Log[x1 x4] + b[11] Log[x1 x5] + b[12] Log[x1 x6] + b[13] Log[x2 x3] + b[14] Log[x2 x4] + b[15] Log[x2 x5] + b[16] Log[x2 x6] + b[17] Log[x3 x4] + b[18] Log[x3 x5] + b[19] Log[x3 x5] + b[20] Log[x3 x6] + b[21] Log[x4 x5] + b[22] Log[x4 x6] + b[23] Log[x5 x6] + b[24] Log[x1]^2 + b[25] Log[x2]^2 + b[26] Log[x3]^2 + b[27] Log[x4]^2 + b[28] Log[x5]^2 + b[29] Log[x6]^2)*)

2.2 Optimization

Optimization means achieving results and fixing problems after making the best use of available resources. Optimization techniques can be classified as conventional and non-conventional. Conventional optimization techniques are only used for continuous and differentiable functions, such as limited variation and Lagrange multipliers. In the present study, Nelder-Mead Algorithm, Differential Evolution Algorithm, Simulated Annealing Algorithm and Random Search Algorithm were chosen to solve the optimization scenarios [13-14].

2.2.1 Nelder Mead Algorithm

Nelder Mead is a simplex method for finding the local minimum point(s) of a function containing several variables. The Nelder Mead method creates a simplex triangle for two variables and compares the function values of this triangle at the vertices. Thus, the optimum point is found. It is an easy and practical method applied in engineering problems [13].

2.2.2 Differential Evolution Algorithm

This technique is based on genetic algorithm. It is an intuitive optimization technique and has a random nature. The productive parameters of this algorithm are population size, crossover and scaling factor. This indicates that you are dealing with a population of solutions rather than repeating them. Among other approaches, differential evolution algorithm is a simple yet powerful technique [14].

2.2.3 Simulated Annealing Algorithm

In this technique, the global optimum value of the function ıs determined. The purpose of the algorithm is to achieve a global optimization and generally used in the computing applications [15].

2.2.4 Random Search Algorithm

Random Search Algorithm can be expressed as a kind of local random search in which each iteration depends on the candidate solution of the previous iteration. It takes samples from the entire search space. In this technique

random search methods are available such as pure random search or uniform general random search. For example, it is known that random search is used for hyper parameter optimization in ANN [16].

2.3 Problem Definition

The wire is arranged as follows to ensure optimum working conditions in WEDM.

- The levels for the various control factors are given in Table 2.
- Electrical discharge process input parameters were modeled with Taguchi design and regression analysis was performed. In Table 3, the parameters related with the reference [17] are given.
- Design variables, where A: Discharge Current, B: Pulse Duration, C: Pulse Frequency, D: Wire Speed, E: Wire Tension, F: Dielectric Flow Rate. These variables have three different levels and given in Table 2. That table is provided from the reference source [17].
- $R^2_{training}$, $R^2_{testing}$ and $R^2_{validation}$ must be greater than 0.90,0.85 and 0.85 respectively . When these conditions are satisfied, it can be concluded that the model is appropriate.
- The validity of the obtained models was checked, and then the suitable models were solved by four different optimization algorithm methods.

2.4 Optimization Scenario

In this optimization problem, the objective function contained kerf (cutting gap) and surface roughness. All design variables are assumed to be real numbers and the search space is continuous. For this case, 16 Amp < Discharge Current (A) < 32 Amp, 3.20 µs < Pulse Duration (B) <12.80µs, 40KHz < Pulse Frequency (C) < 60 KHz, 7.60 m/min < Wire Speed (D) < 9.20 m/min, 1000 g <Wire Tension (E) < 1200 g, 1.20 Bars < Dielectric Flow Rate (F) < 1.40 Bars. The main purpose is to operate the WEDM at an optimal level. Therefore, kerf and surface roughness parameters should be minimized. Mathematically, the boundaries of the objective function can also be obtained with this approach.

Table 2. *Levels for various control factors [17]*

Control Factor	I	II	III
A. Discharge Current (Amp)	16.00	24.00	32.00
B. Pulse Duration (µs)	3.20	6.40	12.80
C. Pulse Frequency (KHz)	40	50	60
D. Wire Speed (m/min)	7.60	8.60	9.20
E. Wire Tension (g)	1000	1100	1200
F. Dielectric Flow Rate (Bars)	1.20	1.30	1.40

Table 3. *Taguchi Experimental Design, input parameters and experimental results [17]*

Expt. No.	A	B	F	C	D	E	R_a(µm)	Kerf(mm)
1	1	1	1	1	1	1	3.68	0.236
2	1	1	2	2	2	2	3.61	0.190
3	1	1	3	3	2	3	3.53	0.161
4	1	2	1	2	2	2	3.82	0.286
5	1	2	2	3	3	3	3.77	0.224
6	1	2	3	1	1	1	3.70	0.217
7	1	3	1	3	3	3	3.86	0.308
8	1	3	2	1	1	1	3.83	0.248
9	1	3	3	2	2	2	3.77	0.204
10	2	1	1	1	2	3	3.64	0.211
11	2	1	2	2	3	1	3.63	0.184
12	2	1	3	3	1	2	3.67	0.256
13	2	2	1	2	3	1	3.89	0.332
14	2	2	2	3	1	2	3.87	0.306
15	2	2	3	1	2	3	3.90	0.372
16	2	3	1	3	1	2	3.86	0.246
17	2	3	2	1	2	3	3.83	0.218
18	2	3	3	2	3	1	3.86	0.278
19	3	1	1	1	3	2	3.73	0.234
20	3	1	2	2	1	3	3.75	0.294
21	3	1	3	3	2	1	3.73	0.254
22	3	2	1	2	1	3	3.80	0.225

23	3	2	2	3	2	1	3.84	0.285
24	3	2	3	1	3	2	3.83	0.253
25	3	3	1	3	2	1	3.99	0.263
26	3	3	2	1	3	2	3.89	0.262
27	3	3	3	2	1	3	3.89	0.259

3. Results and Discussion

It was desired to minimize the surface roughness and kerf values in the wire electrical discharge machine. Various regression models were tested in the literature using $R^2_{training}$, $R^2_{testing}$, $and\ R^2_{validation}$. Multiple regression model types including linear, quadratic, trigonometric, and rational forms were tested. Taguchi design and regression analysis were used to test output-input models in the reference work. In this study, twelve regression models with six parameters were tested. The models are given in Table 1 in detail. In addition, the outputs for the models are given in Table 4 and Table 6. Optimization results and suggested designs are given in Table 5 and Table 7.

Table 5 and Table 7 show that four different optimization algorithms are used. These algorithms are Nelder-Mead Algorithm, Differential Evolution Algorithm, Simulated Annealing Algorithm and Random Search Algorithm. Mathematically, the limits of the objective function can also be obtained with this approach. This approach gives evidence of correct modeling and limitations in optimization after applying twelve different regression models. The results for all algorithms seem close to each other. However, these differences should be analyzed well in sensitive interpretations. The scope of the study is to see the effect of the results of these optimization algorithms on the optimization. Based on this, it can be said that the optimization algorithms in this study give similar values for different algorithms in the results. However, in experimental studies with different data, algorithms can give different results, so it is easier to interpret the effect of the algorithm on optimization. However, it is difficult to explain the difference between optimization algorithms by looking at the results in this study.

The kerf value is minimized for optimum operating conditions. Kerf value is 0.17044 mm. SOLN (Second Order Logarithmic Multiple Nonlinear) as a model. The simulated annealing algorithm was used as a method. Optimal conditions are Discharge Current :32 Amp, Pulse Duration: 3.2 µs, Dielectric Flow Rate: 1.26657 Bars, Pulse Frequency: 60 KHz, Wire Speed:9.2 m/min, Wire Tension: 1200 g.

Table 4. *The results of the regression models and limitation are for kerf.*

Models	$R^2_{training}$	$R^2_{testing}$	$R^2_{validation}$	**Maximum**	**Minimum**
Y=0.345525 + 0.00227546 x1 + 0.00170305 x2 +0.0106114 x3 - 0.00111863 x4 - 0.00218462 x5 - 0.0000948113 x6	0.96762	-1.55346	-1.04871	0.298836	0.199127
Y= (-156.984 + 2.91334 x1 + 4.70894 x2 - 155.444 x3 + 1.88426 x4 - 1.54588 x5 + 0.172973 x6)/(-814.977 + 11.7874 x1 + 21.5156 x2 - 679.797 x3 + 7.04886 x4 + 5.43501 x5 + 0.83685 x6)	0.99741	-278.943	-1.0293	178469.	$-1.16373*10^{12}$
Y=3.02691 + 0.0852935 x1 - 0.000278251 x1^2 + 0.0220959 x2 - 0.000478143 x1 x2 - 0.00253284 x2^2 - 3.72551 x3 + 0.0299919 x1 x3 - 0.0269791 x2 x3 + 1.2682 x3^2 + 0.0349188 x4 - 0.000104581 x1 x4 + 0.000716035 x2 x4 - 0.000415591 x4^2 + 0.0622959 x5 - 0.00214178 x1 x5 + 0.00365543 x2 x5 - 0.00495281 x5^2 - 0.00414701 x6 - 0.0000749325 x1 x6 +2.64107*10^-6 x6^2	0.987461	-4.64949	-0.0116655	0.512067	-0.0131406
Y=(1.00142 + 1.02142 x1 - 0.363206 x1^2 + 1.01119 x2 + 2.51615 x1 x2 - 2.03674 x2^2 + 0.996731 x3 + 2.02719 x1 x3 + 1.87877 x2 x3 + 0.989473 x3^2 + 1.00466 x4 + 8.66948 x1 x4 + 5.29075 x2 x4 - 2.41314 x4^2 + 1.0293 x5 + 3.7472 x1 x5 + 3.58219 x2 x5 + 1.39927 x5^2 + 1.65865 x6 + 5.41413	0.969526	-0.310494	-0.880369	0.269572	0.179999

x1 x6 - 0.0653058 x6^2)/(0.999656 + 0.998974 x1 + 1.55153 x1^2 + 1.00405 x2 + 2.47433 x1 x2 + 1.82439 x2^2 + 1.0005 x3 + 1.99323 x1 x3 + 2.05869 x2 x3 + 1.0018 x3^2 + 0.991958 x4 + 0.534298 x1 x4 + 2.55489 x2 x4 + 1.13551 x4^2 + 0.993309 x5 + 1.74626 x1 x5 + 1.8483 x2 x5 + 0.910865 x5^2 + 0.842715 x6 + 21.4831 x1 x6 - 0.239944 x6^2)					
Y=2.6147 + 0.0248117 Cos[x1] + 0.0767145 Cos[x2] - 0.695018 Cos[x3] + 0.00804462 Cos[x4] + 0.00206104 Cos[x5] - 0.0623113 Cos[x6] - 0.0158866 Sin[x1] - 0.485028 Sin[x2] - 2.23478 Sin[x3] + 0.0179596 Sin[x4] + 0.0467603 Sin[x5] + 0.00575167 Sin[x6]	0.983099	0.922505	-4.75779	0.943884	-0.320025
Y=2.6147 + 0.0248117 Cos[x1] + 0.0767145 Cos[x2] - 0.695018 Cos[x3] + 0.00804462 Cos[x4] + 0.00206104 Cos[x5] - 0.0623113 Cos[x6] - 0.0158866 Sin[x1] - 0.485028 Sin[x2] - 2.23478 Sin[x3] + 0.0179596 Sin[x4] + 0.0467603 Sin[x5] + 0.00575167 Sin[x6]	0.992522	-5.13909	-8.59265	$3.7212*10^{7}$	$-5.94437*10^{6}$
Y=0.0328006 + 0.035645 Cos[x1] + 0.0325077 Cos[x1]^2 + 0.0757116 Cos[x2] + 0.0400001 Cos[x2]^2 - 0.741854 Cos[x3] + 1.31834 Cos[x3]^2 + 0.00877994 Cos[x4] + 0.0394002 Cos[x4]^2 - 0.000300729 Cos[x5] + 0.0403801 Cos[x5]^2 + 0.0301413 Cos[x6] + 0.0290802 Cos[x6]^2 - 0.0304481 Sin[x1] - 0.471283 Sin[x2] + 0.027312 Sin[x3] + 0.0506393 Sin[x3]^2 + 0.00332714 Sin[x4] + 0.0721788 Sin[x4]^2 + 0.0377993 Sin[x5] + 0.0511693 Sin[x5]^2 - 0.000961744 Sin[x6] + 0.097492 Sin[x6]^2	0.983099	0.92225	-4.75779	0.838918	-0.433362
Y=(-0.143231 + 1.02503 Cos[x1] + 0.319877 Cos[x1]^2 + 1.33965 Cos[x2] + 1.64897 Cos[x2]^2 - 0.686355 Cos[x3] + 0.626178 Cos[x3]^2 + 0.337058 Cos[x4] + 0.442023 Cos[x4]^2 + 0.667737 Cos[x5] + 0.198311 Cos[x5]^2 + 0.172114 Cos[x6] + 0.375179 Cos[x6]^2 + 2.71112 Sin[x1] - 4.19607 Sin[x2] + 0.0334958 Sin[x3] + 0.461181 Sin[x3]^2 + 0.187331 Sin[x4] + 0.414746 Sin[x4]^2 + 0.783651 Sin[x5] + 0.658458 Sin[x5]^2 + 0.190198 Sin[x6] + 0.48159 Sin[x6]^2)/(1.50951 + 3.28362 Cos[x1] + 2.51938 Cos[x1]^2 + 2.60966 Cos[x2] + 1.00835 Cos[x2]^2 + 2.13008 Cos[x3] + 1.45514 Cos[x3]^2 + 1.24312 Cos[x4] + 1.49287 Cos[x4]^2 + 2.84951 Cos[x5] + 0.669053 Cos[x5]^2 + 1.64504 Cos[x6] + 1.67608 Cos[x6]^2 + 10.5281 Sin[x1] + 2.57822 Sin[x2] + 1.27688 Sin[x3] + 2.10872 Sin[x3]^2 + 0.812532 Sin[x4] + 1.01664 Sin[x4]^2 + 1.47664 Sin[x5] + 1.84045 Sin[x5]^2 + 1.11108 Sin[x6] + 0.83343 Sin[x6]^2)	0.99487	-2.43018	-4.29465	$7.71308*10^{6}$	$-2.57775*10^{7}$

2.6147 + 0.0248117 Cos[x1] + 0.0767145 Cos[x2] - 0.695018 Cos[x3] + 0.00804462 Cos[x4] + 0.00206104 Cos[x5] - 0.0623113 Cos[x6] - 0.0158866 Sin[x1] - 0.485028 Sin[x2] - 2.23478 Sin[x3] + 0.0179596 Sin[x4] + 0.0467603 Sin[x5] + 0.00575167 Sin[x6]	0.969421	-1.71268	-0.755777	0.304101	0.191605
(-410.542 + 505.756 Log[x1] + 86.3088 Log[x2] + 137.106 Log[x3] + 168.48 Log[x4] - 1260.57 Log[x5] + 104.764 Log[x6])/(-100.648 + 2029.13 Log[x1] + 468.664 Log[x2] - 344.646 Log[x3] + 358.247 Log[x4] - 4832.5 Log[x5] + 299.616 Log[x6])	0.996957	-17.7241	-2966.27	12704.9	-307377.
30.344 + 0.765363 Log[x1] - 0.221966 Log[x1]^2 + 0.509759 Log[x2] - 0.130349 Log[x2]^2 + 0.378032 Log[x1 x2] - 3.01852 Log[x3] + 2.01673 Log[x3]^2 + 0.639298 Log[x1 x3] + 0.355116 Log[x2 x3] + 0.616684 Log[x4] - 0.164074 Log[x4]^2 + 0.342368 Log[x1 x4] + 0.339301 Log[x2 x4] + 0.531829 Log[x3 x4] + 2.07915 Log[x5] - 1.36013 Log[x5]^2 + 0.612108 Log[x1 x5] + 0.711383 Log[x2 x5] + 3.25295 Log[x3 x5] + 0.518864 Log[x4 x5] - 2.90909 Log[x6] + 0.805314 Log[x6]^2 - 1.30757 Log[x1 x6] - 1.802 Log[x2 x6] - 2.71383 Log[x3 x6] - 1.12419 Log[x4 x6] - 1.59307 Log[x5 x6]	0.983099	0.92225	-4.75779	0.363967	0.139315
(0.392182 + 2.6288 Log[x1] + 3.23866 Log[x1]^2 + 7.93825 Log[x2] - 11.1651 Log[x2]^2 + 9.56705 Log[x1 x2] + 2.15288 Log[x3] + 1.93372 Log[x3]^2 + 3.78168 Log[x1 x3] + 9.09114 Log[x2 x3] - 0.31849 Log[x4] - 0.943493 Log[x4]^2 + 1.31031 Log[x1 x4] + 6.61976 Log[x2 x4] + 0.834391 Log[x3 x4] - 0.808902 Log[x5] - 4.41187 Log[x5]^2 + 0.819894 Log[x1 x5] + 6.12935 Log[x2 x5] + 0.687958 Log[x3 x5] - 2.12739 Log[x4 x5] - 1.3626 Log[x6] - 1.6747 Log[x6]^2 + 0.266192 Log[x1 x6] + 5.57565 Log[x2 x6] - 0.209723 Log[x3 x6] - 2.68109 Log[x4 x6] - 3.17151 Log[x5 x6])/(0.981338 + 3.25945 Log[x1] + 19.6328 Log[x1]^2 - 0.569116 Log[x2] + 4.65743 Log[x2]^2 + 1.69033 Log[x1 x2] + 0.303267 Log[x3] + 0.565446 Log[x3]^2 + 2.56272 Log[x1 x3] - 1.26585 Log[x2 x3] + 0.769713 Log[x4] - 0.298893 Log[x4]^2 + 3.02916 Log[x1 x4] - 0.799403 Log[x2 x4] + 0.0729798 Log[x3 x4] + 0.432774 Log[x5] - 1.1629 Log[x5]^2 + 2.69222 Log[x1 x5] - 1.13634 Log[x2 x5] - 0.527919 Log[x3 x5] + 0.202487 Log[x4 x5] + 0.604482 Log[x6] - 3.80114 Log[x6]^2 + 2.86393 Log[x1 x6] - 0.964634 Log[x2 x6] - 0.0922513 Log[x3 x6] + 0.374195 Log[x4 x6] + 0.0372559 Log[x5 x6])	0.984678	0.842674	-11.7328	0.404415	0.0481186

Table 5. *Results of optimization problems for the four models selected for kerf minimization.*

Objective Functions	Constraints	Optimization Algorithm	Kerf(mm) Minimization	Suggested Design
FOTN	16 < x1 < 32, 3.2 < x2 <12.8, 1.2 < x3 < 1.4 ,40 < x4 < 60, 7.6 < x5 < 9.2, 1000 < x6 < 1200	MDE	-0.320025	x1 -> 21.4216, x2 -> 8.01085, x3 -> 1.26928, x4 -> 48.2736, x5 -> 9.2, x6 -> 1200.
		MSA	-0.320025	x1 -> 27.7048, x2 -> 8.01085, x3 -> 1.26928, x4 -> 54.5567, x5 -> 9.2, x6 -> 1181.15
		MRS	-0.320025	x1 -> 27.7048, x2 -> 8.01085, x3 -> 1.26928, x4 -> 41.9904, x5 -> 9.2, x6 -> 1086.9
		MNM	-0.320025	x1 -> 27.7048, x2 -> 8.01085, x3 -> 1.26928, x4 -> 54.5567, x5 -> 9.2, x6 -> 1105.75
SOTN	16 < x1 < 32, 3.2 < x2 < 12.8,1.2 < x3 < 1.4 ,40 < x4 < 60, 7.6 < x5 < 9.2,1000 < x6 < 1200	MDE	-0.433362	x1 -> 27.0769, x2 -> 7.99065, x3 -> 1.27036, x4 -> 59.735, x5 -> 9.2, x6 -> 1077.56
		MSA	-0.433362	x1 -> 27.0769, x2 -> 7.99065, x3 -> 1.27036, x4 -> 47.1687, x5 -> 9.2, x6 -> 1165.53
		MRS	-0.433362	x1 -> 27.0769, x2 -> 7.99065, x3 -> 1.27036, x4 -> 59.735, x5 -> 9.2, x6 -> 1014.73
		MNM	-0.415825	x1 -> 27.0769, x2 -> 7.99065, x3 -> 1.27036, x4 -> 50.2068, x5 -> 9.2, x6 -> 1064.99
SOLN	16 < x1 < 32, 3.2 < x2 < 12.8, 1.2 < x3 < 1.4 ,40 < x4 < 60, 7.6 < x5 < 9.2, 1000 < x6 < 1200	MDE	0.139315	x1 -> 16., x2 -> 3.2, x3 -> 1.26657, x4 -> 60., x5 -> 9.2, x6 -> 1200.
		MSA	0.17044	x1 -> 32., x2 -> 3.2, x3 -> 1.26657, x4 -> 60., x5 -> 9.2, x6 -> 1200.
		MRS	0.149927	x1 -> 16., x2 -> 12.8, x3 -> 1.26657, x4 -> 60., x5 -> 9.2, x6 -> \1200.
		MNM	0.139315	x1 -> 16., x2 -> 3.2, x3 -> 1.26657, x4 -> 60., x5 -> 9.2, x6 -> 1200.
SOLNR	16 < x1 < 32, 3.2 < x2 < 12.8,1.2 < x3 < 1.4 ,40 < x4 < 60, 7.6 < x5 < 9.2, 1000 < x6 < 1200	MDE	0.0481184	x1 -> 16., x2 -> 3.2, x3 -> 1.2, x4 -> 60., x5 -> 9.2, x6 -> 1200.
		MSA	0.0481207	x1 -> 16., x2 -> 3.2, x3 -> 1.2, x4 -> 59.9994, x5 -> 9.2, x6 -> 1200.
		MRS	0.0481185	x1 -> 16., x2 -> 3.2, x3 -> 1.2, x4 -> 60., x5 -> 9.2, x6 -> 1200.
		MNM	0.0481186	x1 -> 16., x2 -> 3.2, x3 -> 1.2, x4 -> 60., x5 -> 9.2, x6 -> 1200.

Table 6. *The results of the regression models and limitation are for surface roughness.*

Model	Maximum	Minimum	$R^2_{training}$	$R^2_{testing}$	$R^2_{validation}$
4.06381 + 0.104384 Log[x1] + 0.156206 Log[x2] - 0.218486 Log[x3] - 0.0115373 Log[x4] + 0.0443204 Log[x5] - 0.126955 Log[x6]	0.999779	0.865904	0.89335	3.9628	3.60393

Table 7. *Results of optimization problems for the one model selected for surface roughness minimization.*

Objective Functions	**Constraints**	**Optimization Algorithm**	**Surface Rouhness (µm) Minimization**	**Suggested Design**
FOLN	16 < x1 < 32, 3.2 < x2 <12.8, 1.2 < x3 < 1.4 ,40 < x4 < 60, 7.6 < x5 < 9.2, 1000 < x6 < 1200	MDE	3.60393	x1 -> 16., x2 -> 3.2, x3 -> 1.4, x4 -> 60., x5 -> 7.6, x6 -> 1200.
		MSA	3.60394	x1 -> 16.0001, x2 -> 3.20001, x3 -> 1.4, x4 -> 59.9918, x5 -> 7.60005, x6 -> 1199.99
		MRS	3.60393	x1 -> 16., x2 -> 3.2, x3 -> 1.4, x4 -> 59.9994, x5 -> 7.60001, x6 -> 1200.
		MNM	3.60393	x1 -> 16., x2 -> 3.2, x3 -> 1.4, x4 -> 59.9999, x5 -> 7.6, x6 -> 1200.

When the tables are examined, the suitability of the regression models is very important in optimizing. Because, in fact, every experiment has a working principle suitable for maximizing or minimizing in accordance with the working dynamics.

The surface roughness value is minimized for optimum operating conditions. Surface roughness value is 3.60393 µm. FOLN (First Order Logarithmic Multiple Nonlinear) as a model The differential evolution was used as a method. Optimal conditions are Discharge Current :16 Amp, Pulse Duration: 3.2 µs, Dielectric Flow Rate: 1.4 Bars, Pulse Frequency: 60 KHz, Wire Speed: 7.6 m/min, Wire Tension: 1200 g.

For surface roughness and kerf, the results fit the input ranges. Provided the training, testing and validation phase for surface roughness. Provided the training and testing phase for Kerf. Looking at the tables in general, it can be seen that the study was successful (Table 4, Table 5, Table 6 and Table 7).

4. Conclusions

In this study, important processing parameters were tried to be determined separately for performance measurements such as surface roughness and kerf in the WEDM process. It has been seen that factors such as discharge current, pulse frequency and pulse duration and their interactions play an important role in rough cutting for kerf and surface roughness minimization.

Taguchi's experimental design method and multiple regression models are used to obtain the optimum parameter combination for minimization of kerf and surface roughness. The data separated as 80%, 15% and 5% in the modeling were randomly selected. This increased the reliability of the experiment. Thus, there was no accumulation in a certain number range. The most important part of the work is to check the accuracy of the limits of the proposed input parameters in the minimization results. This gives a great idea of the accuracy of the model. After using twelve different regression models, using four different optimization algorithms (Nelder-Mead Algorithm, Differential Evolution Algorithm, Simulated Annealing Algorithm and Random Search Algorithm) increased the accuracy of the optimization results.

This work can be extended in the future for different processing parameters and outputs. In addition, the work can be further improved with hybrid regression modeling techniques.

Declaration of Interest

The authors declare that there is no conflict of interest.

References

[1] Khatri, Bharat C., and Rathod, Pravin P. (2017). "Investigations on the performance of concentric flow dry wire electric discharge machining (WEDM) for thin sheets of titanium alloy." Int J Adv Manuf Technol Springer-Verlag London , 92,1945–1954.

[2] Mouralova, K., Kovar, J., Klakurkova, L.,and Prokes, T. (2018). "Effect of Width of Kerf on Machining Accuracy and Subsurface Layer After WEDM." JMEPEG ASM International, 27(4), 1908-1916

[3] Han, F., Jiang, J., Yu, D. (2006). "Influence of machining parameters on surface roughness in finish cut of WEDM." Int J Adv Manuf Technol Springer-Verlag London Limited, 34, 538–546.

[4] Saha, A., and Mondal, S. C. (2016). "Experimental investigation and modelling of WEDM process for machining nano-structured hardfacing material. " J Braz. Soc. Mech. Sci. Eng. The Brazilian Society of Mechanical Sciences and Engineering 2, 39, 3439–3455.

[5] Kumar, A., Grover N., Manna, A., Kumar, R., Chohan J. S., Singh, S., Singh, S., and Prunchu, C. L. (2021). "Multi-Objective Optimization of WEDM of Aluminum Hybrid Composites Using AHP and Genetic Algorithm." Arabian Journal for Science and Engineering Crown 2.

[6] Shihab, K. (2018). "Optimization of WEDM Process Parameters for Machining of Friction-Stir-Welded 5754 Aluminum Alloy Using Box–Behnken Design of RSM." Arabian Journal for Science and Engineering King Fahd University of Petroleum & Minerals , 43, 5017-5027.

[7] Ming, W., Hou, J., Zhang, Z., Huang, H., Xu, Z., Zhang, G., and Huang, Y. (2015). "Integrated ANN-LWPA for cutting parameter optimization in WEDM." Int J Adv Manuf Technol Springer-Verlag London , 84, 1277–1294.

[8] Majumder, H., and Maity, K. P. (2018) "Predictive Analysis on Responses in WEDM of Titanium Grade 6 Using General Regression Neural Network (GRNN) and Multiple Regression Analysis (MRA)." Silicon Springer Science+Business Media B.V. 2018, 10,1763–1776.

[9] Phate, M. R., Toney, S. B., and Phate, V. R. (2020). "Multi-parametric Optimization of WEDM Using Artificial Neural Network (ANN)-Based PCA for Al/SiCp MMC." J. Inst. Eng. India Ser. C The Institution of Engineers (India), 102(1), 169–181.

[10] Manjaiah, M., Laubscher, R. F., Kumar, A., and Basavarajappa, S. (2016). "Parametric optimization of MRR andsurface roughness in wire electro dischargemachining (WEDM) of D2 steel using Taguchi-based utility approach." International Journal of Mechanical and Materials Engineering Springer-Verlag London Limited, 11(7), 237-248.

[11] Polatoğlu, I., Aydın, L., Nevruz, B. Ç.,and Öze, S. (2020). "A Novel Approach for the Optimal Design of a Biosensor." Analytical Letters Taylor & Francis Group, LLC.

[12] Akcair, M., Savran, M., Aydın, L., Ayakdas, O., Ozturk, S.,and Kucukdogan, N. (2019) "Optimum design of anti-buckling behaviour of graphite/epoxy laminated composites by differential evolution and simulated annealing method. " Research on Engineering Structures and Materials, 5, 175–88.

[13] Zhang, Y., Price, C. J., Coope, I. D., Byatt, D. (2002). "A Convergent Variant of the Nelder–Mead Algorithm." JOURNAL OF OPTIMIZATION THEORY AND APPLICATIONS Plenum Publishing Corporation, 113(1), 5-19.

[14] Majumder, A., Das, A., Das, P. Kr. (2016). "A standard deviation based firefly algorithm for multi-objective optimization of WEDM process during machining of Indian RAFM steel." Neural Comput & Applic The Natural Computing Applications, 29, 665–677.

[15] Somashekhar, K. P., Mathew, J., & Ramachandran, N. (2012). "A feasibility approach by simulated annealing on optimization of micro-wire electric discharge machining parameters." Int J Adv Manuf Technol Springer-Verlag London, 61, 1209–1213.

[16] Kaelo, P., and Alİ, M. M. (2006). "Some Variants of the Controlled Random Search Algorithm for Global Optimization." JOURNAL OF OPTIMIZATION THEORY AND APPLICATIONS Springer Science+Business Media, Inc., 130(2), 253-264.

[17] Mahapatra, S. S., and Patnaik, A. (2007). "Optimization of wire electrical discharge machining (WEDM) process parameters using Taguchi method." The International Journal of Advanced Manufacturing Technology, 34, 911-925